Search for SUSY in events with a photon, jets, b-jets, and missing transverse momentum in p-p collisions at 13 TeV

Thesis endorsement

Vinay Hegde
Thesis Supervisor: Dr. Seema Sharma

Indian Institute of Science Education & Research, Pune

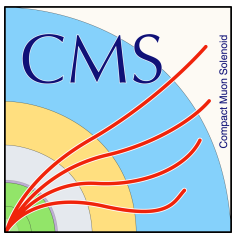

About the work

- **Thesis title**: Search for supersymmetry in events with a photon, jets, b-jets, and missing transverse momentum.
- CMS CADI link: SUS-18-002
- Arxiv: 1901.06726
- Paper is submitted to EPJC and addressed minor comments from referee.

- Requesting to approve plots which are not public. They are shown as

  For thesis

Introduction

- This analysis is a search for SUSY with GMSB scenarios.
- Final state: at least 1 photon, p_T^{miss}, jets and b- jets.
- Gravitino (G~)
  - super-partner of G & is the LSP.
  - interacts weakly giving p_T^{miss} signature.

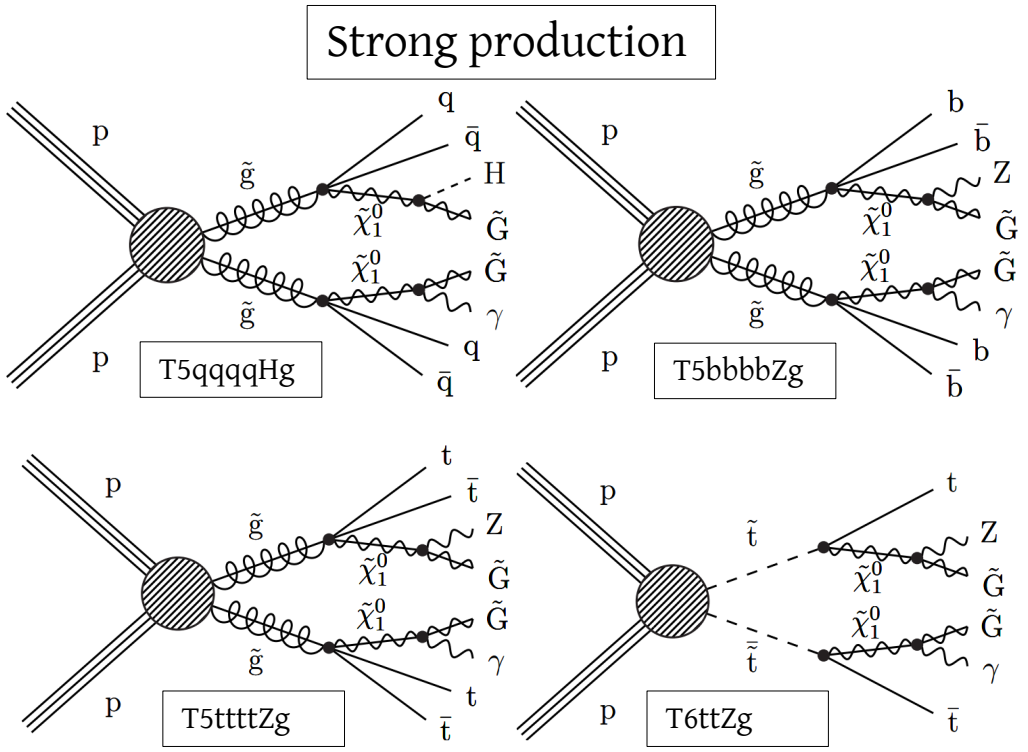

Event selections

- >=1 photon with pT > 100 GeV
- p_T^{miss}> 200 GeV
- >=2 jets.
- Veto e/μ and isolated tracks.
- HTγ = sum Pt of jets + photon Pt > 500 GeV if photon Pt > 190GeV.
- HTγ > 800GeV if Photon Pt > 100GeV.
- Angular cut: ΔΦ(MET, Jet1) and ΔΦ(MET,Jet2) > 0.3.
- Triggers: “HLT_Photon90_CaloIdL_PFHT600” **OR** “HLT_Photon165_HE10”

MC event yields in various regions

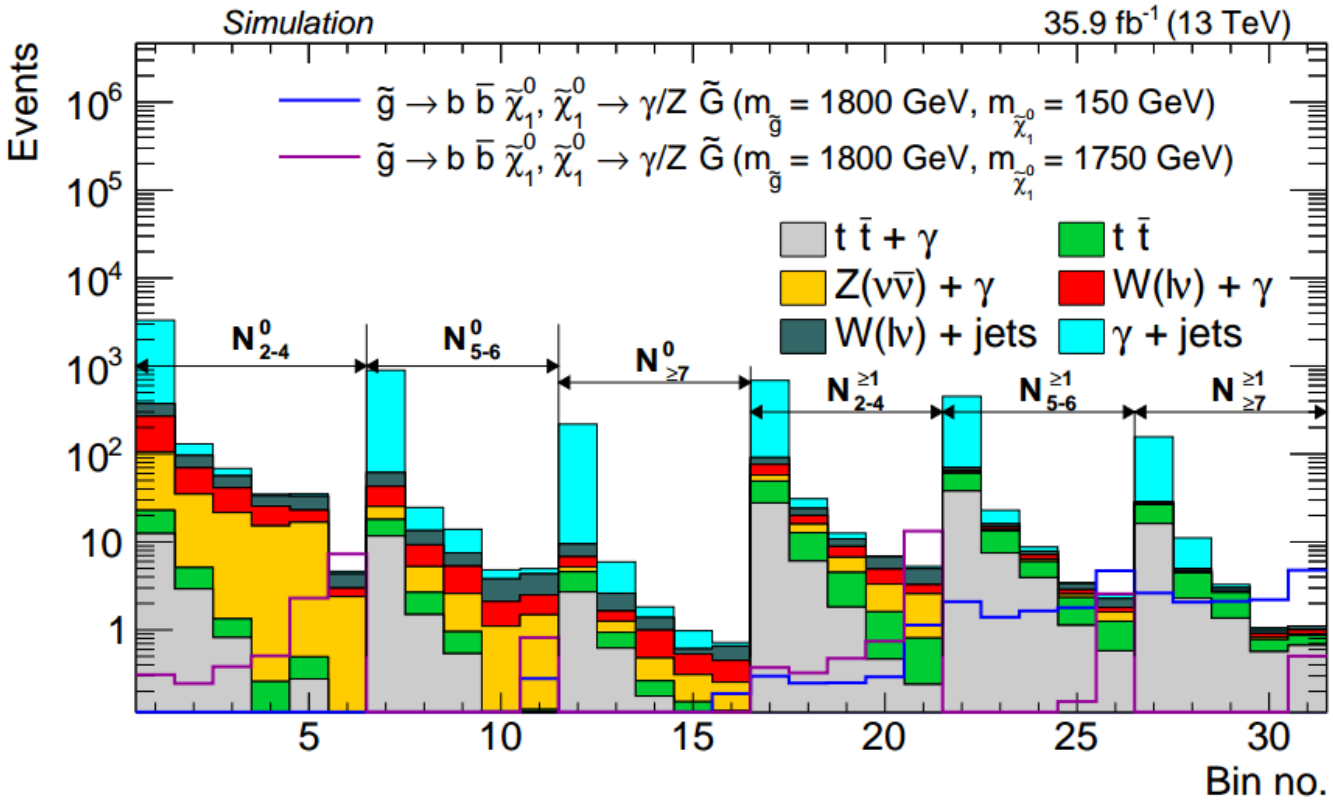

For thesis

p_T^{miss} bins in each of $N^{b\text{-}tags}_{jets}$: 200-270, 270-350, 350-450, 450-750, >=750 : for $N^0_{2\text{-}4}$. 200-270, 270-350, 350-450, >=450 for other N^i_j

FIGURE 3.8: Distributions of events after baseline selection. Filled, stacked histograms represent SM backgrounds, taken directly from simulation, open histograms show two examples of T5bbbbZG signals, one with a high mass (1750 GeV) NLSP and one with a low mass (150 GeV) NLSP. The gluino mass for both signals is 1800 GeV. The lowest p_T^{miss} bin is not used for final limit calculations.

Photon165 Trigger efficiency

For thesis

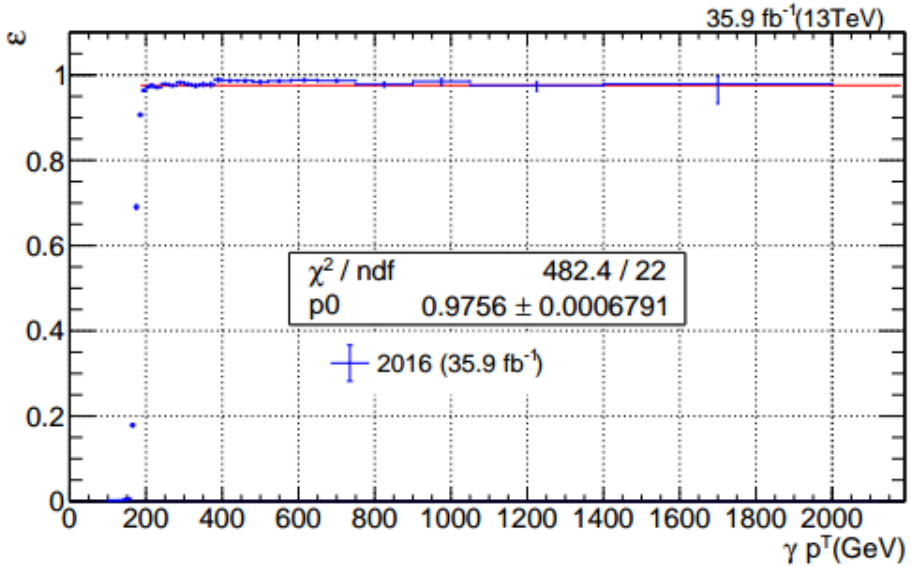

For thesis

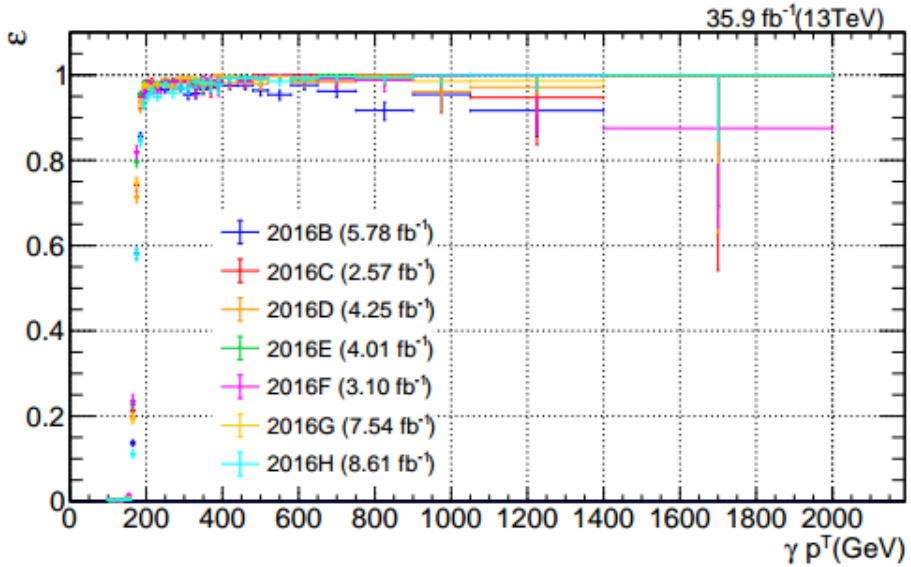

FIGURE 3.2: Efficiency of Photon165 trigger versus p_T^γ for all eras (left) and split by eras (right).

HTxPhoton Trigger efficiency

For thesis: all plots

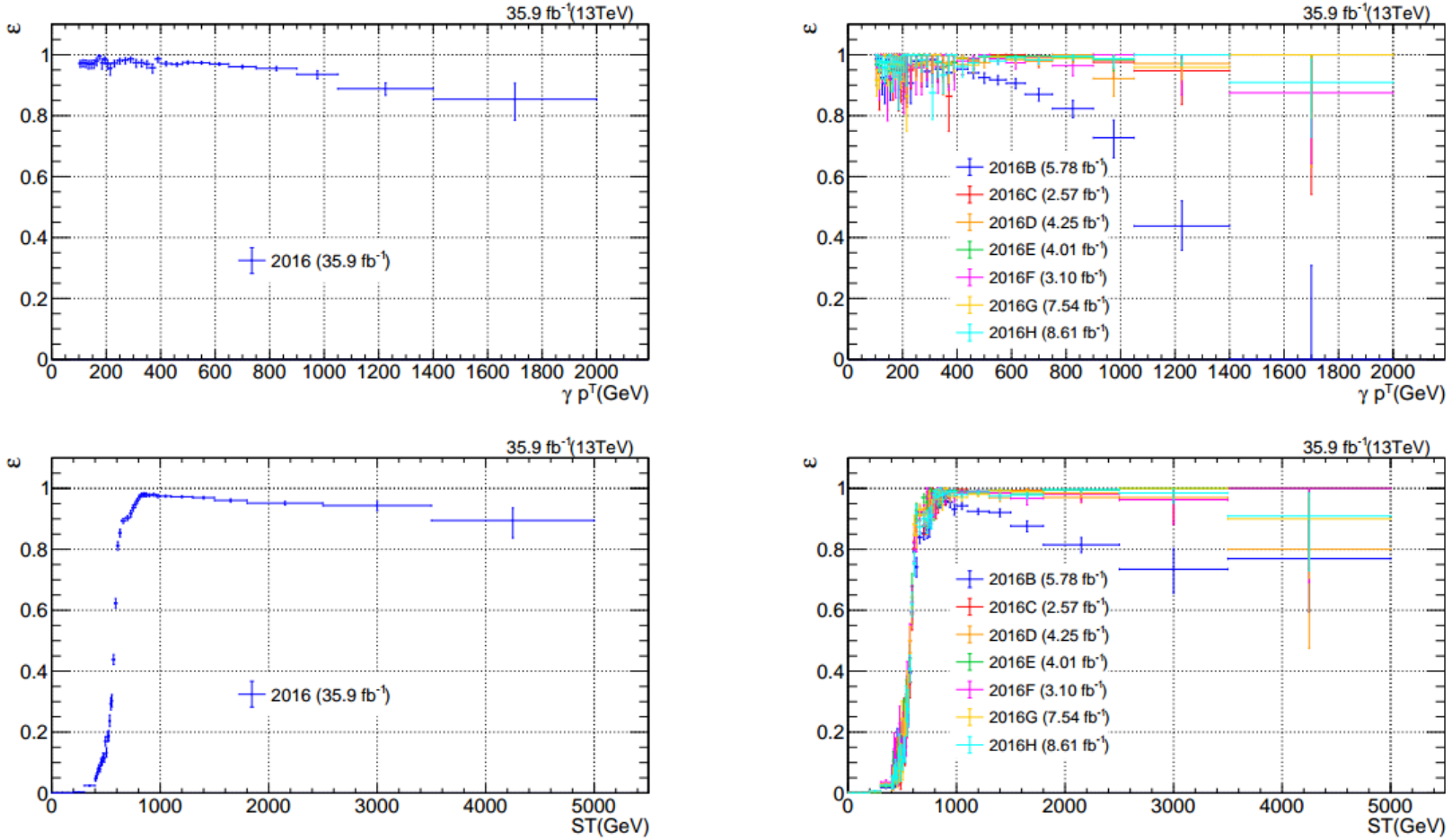

FIGURE 3.3: Efficiency of Photon90_PFHT600 trigger versus p_T^γ (top) and H_T^γ (bottom) for all eras (left) and split by eras (right).

Photon165 || HTxPhoton Trigger efficiency

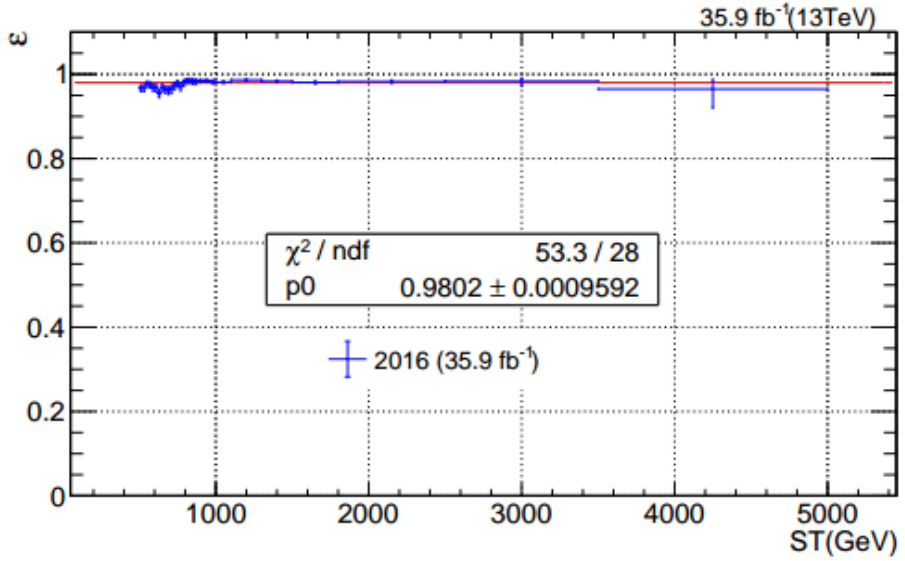

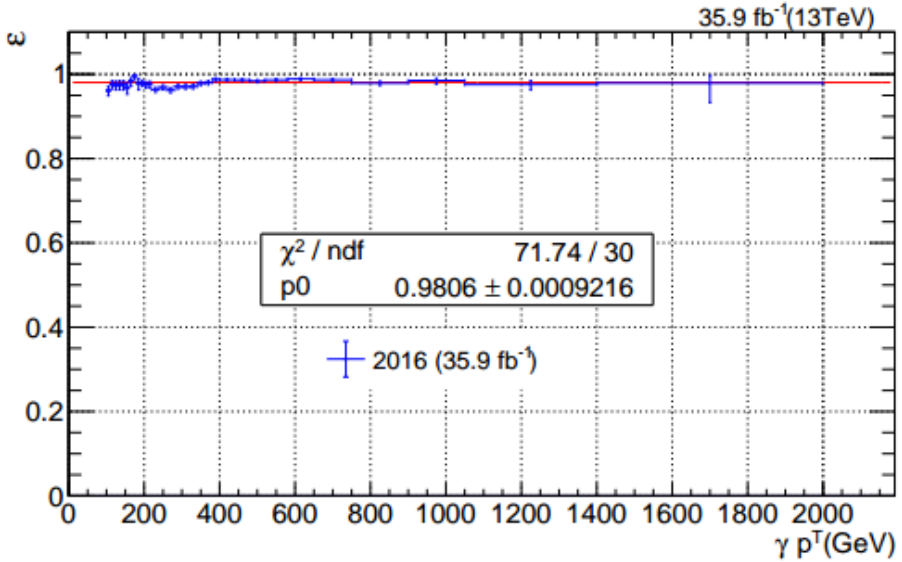

FIGURE 3.4: Efficiency of the OR of the Photon165 and Photon90_PFHT600 triggers versus H_{T}^{γ} (left) and p_{T}^{γ} (right).

For thesis: all plots

Photon165 || HTxPhoton Trigger efficiency for tight ID electrons

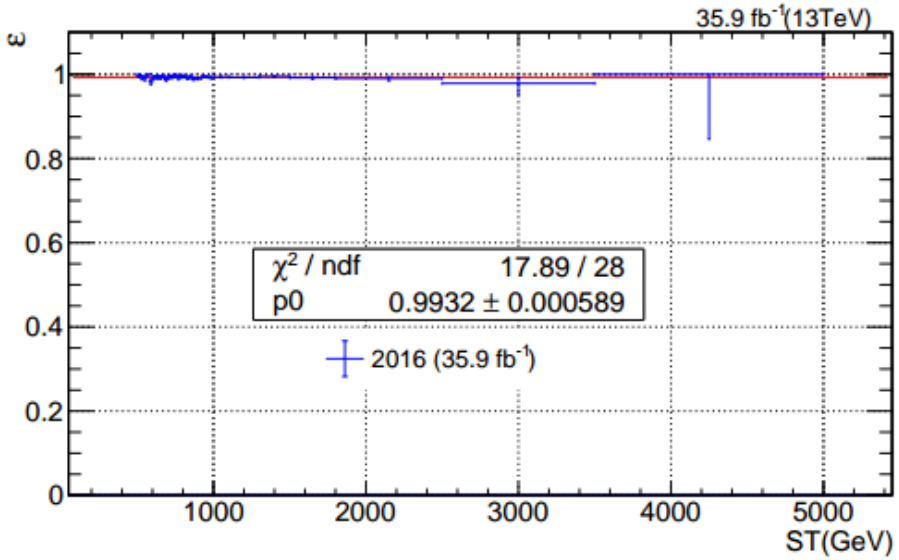

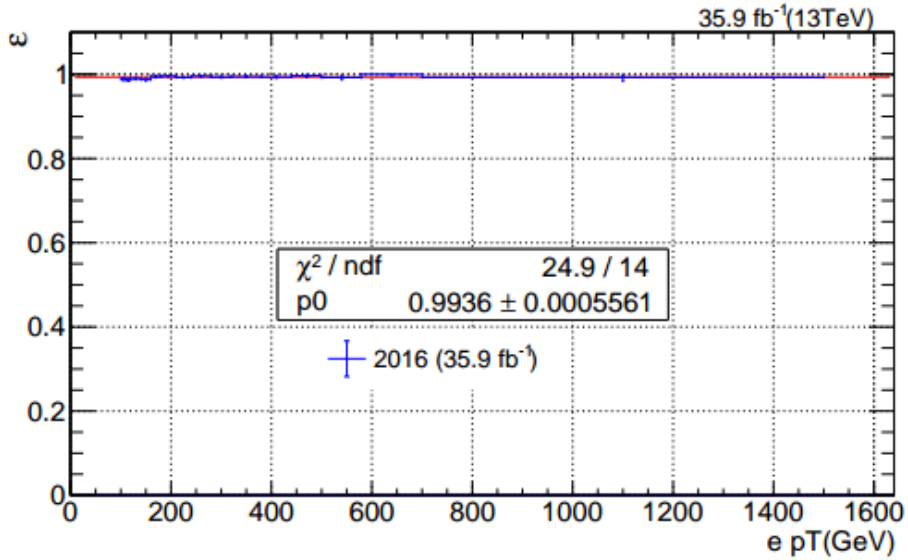

FIGURE 3.5: Efficiency of the OR of the Photon165 and Photon90_PFHT600 versus H_T^γ (left) and p_T^γ (right) for events with one tight electron.

For thesis: all plots

Triggers for 0 photon events

For thesis: all plots

- PFHT and CaloJet triggers are used to select events with 0 photon which are used in the validation of γ + jets background estimation method.

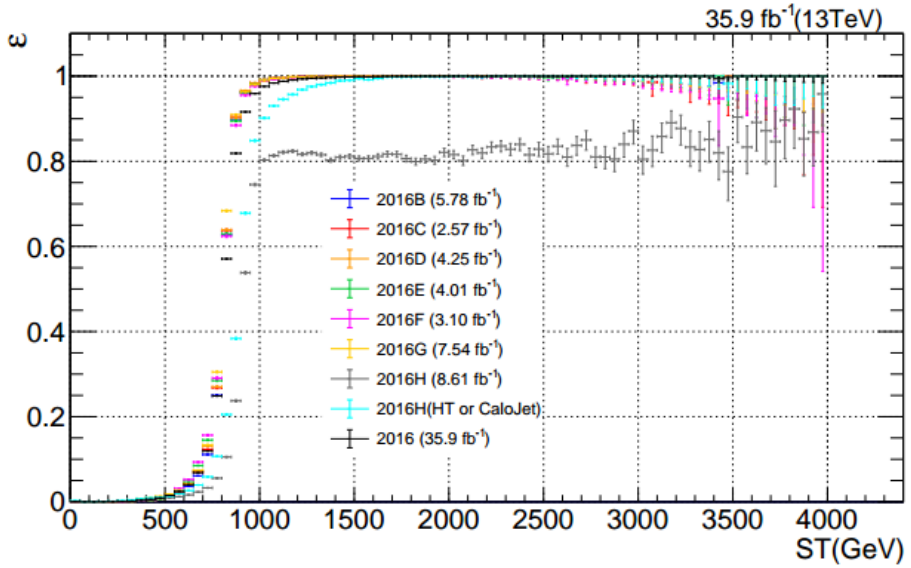

FIGURE 3.6: Efficiency of HLT_PFHT800 trigger for eras B-G, and HLT_PFHT900 OR HLT_CaloJet500_NoJetID for era H for zero photon events.

Optimization studies

- Studied various strategies to optimize the analysis. These plots show the expected exclusions using different strategies.

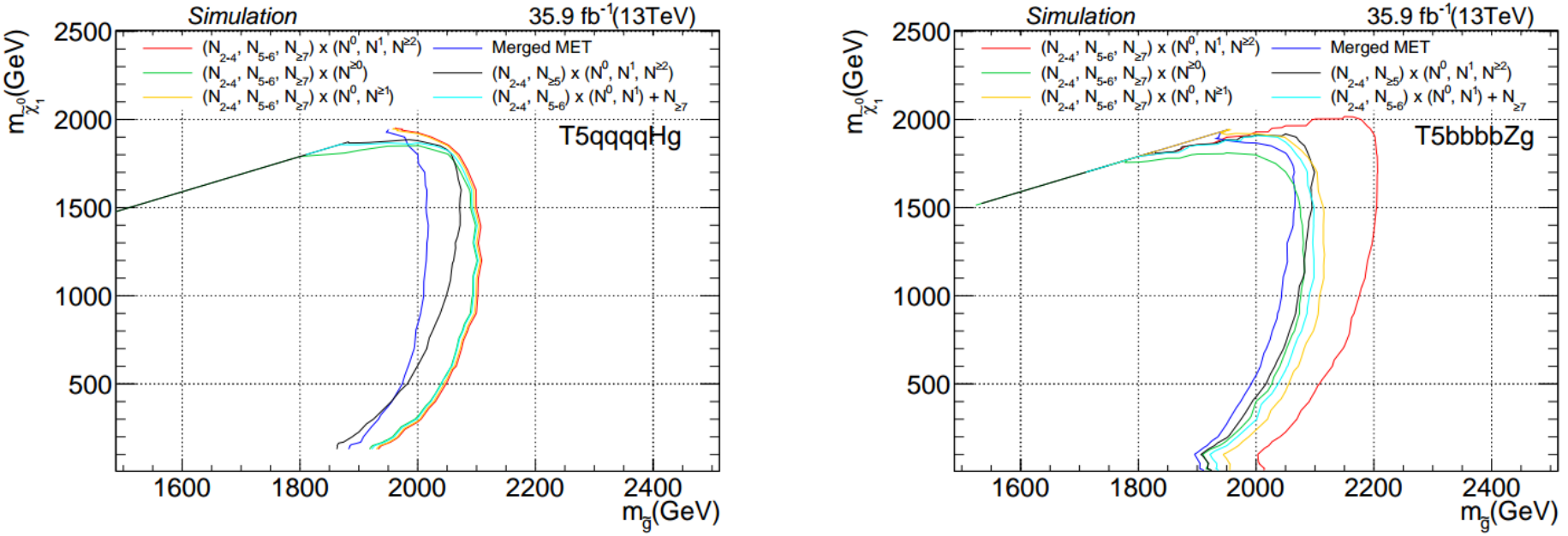

FIGURE 3.9: Expected exclusion curves for different types of binning for T5qqqqHG (left) and T5bbbbZG (right). In the legends, subscript j in N_j^i refers to number of jets and superscript i refers to number of b-tagged jets. The red curve corresponds to 63 search bins defined as (N_{jets} = 2-4, 5-6, $\geq$ 7) $\times$ ($N_{\text{b-jets}}$ = 0, 1, $\geq$ 2) $\times$ (7 p_T^{miss} bins). Other curves are obtained by combining these 63 bins in either N_{jets} or $N_{\text{b-jets}}$ or p_T^{miss} or any combination of these variables. The final binning of the analysis is based on orange curve defined as (N_{jets} = 2-4, 5-6, $\geq$ 7) $\times$ ($N_{\text{b-jets}}$ = 0, $\geq$ 1) $\times$ (7 p_T^{miss} bins).

Lost lepton closures

- Lost lepton and hadronic τ background is estimated using transfer factor (TF) method.
- TF is the ratio of lost lepton (+hadronic τ) events to found lepton events derived from MC.
- These plots show the closure for lost electron and lost muon + hadronic τ contributions using MC.

For thesis

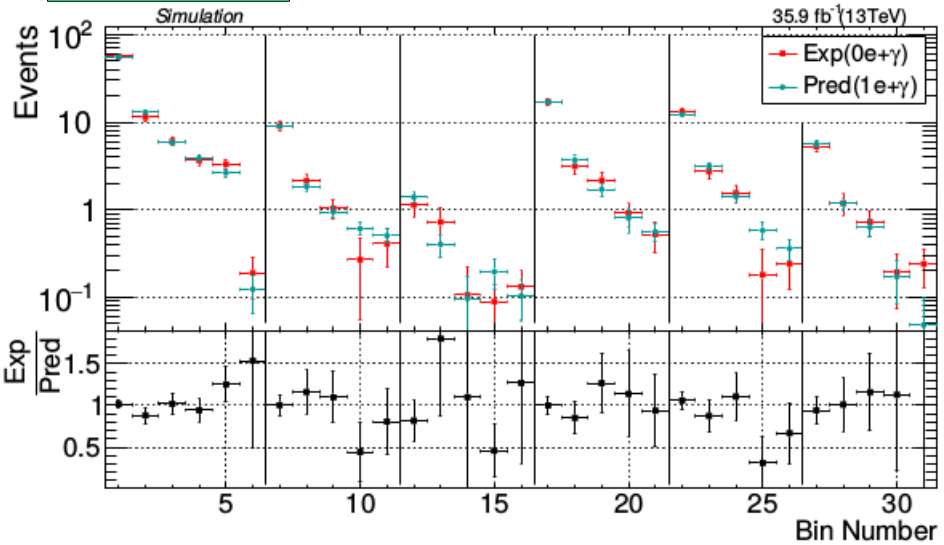

For thesis

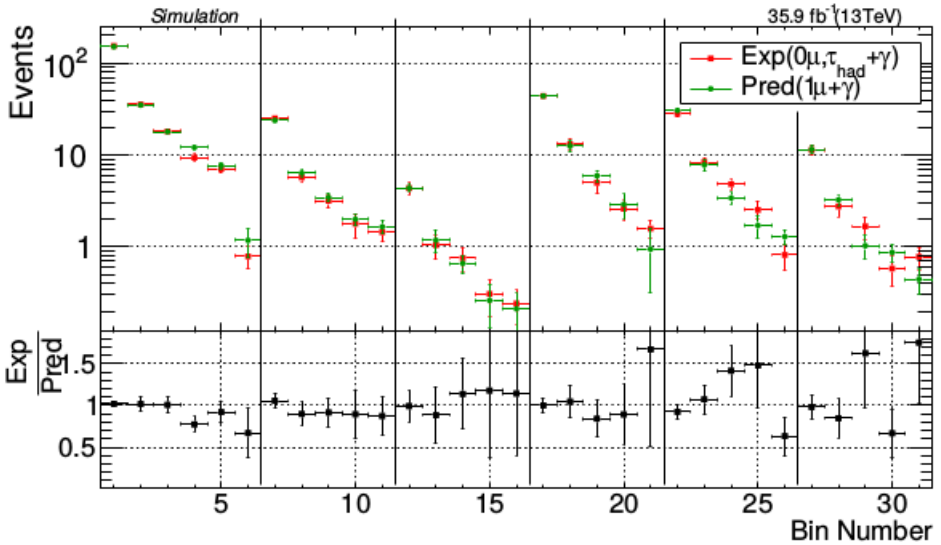

FIGURE 4.12: Expected closure of lost electron (left) and lost $\mu + \tau_{had}$ (right) predictions where simulated event yields are treated like data.

Control regions for lost lepton and hadronic τ estimation

- For estimation of lost electron e+γ control region is used.
- For estimation of lost μ + hadronic τ, muon+γ control region is used.
- Next few slides show data-MC comparisons in these control regions.

Lost lepton control regions

For thesis: all plots

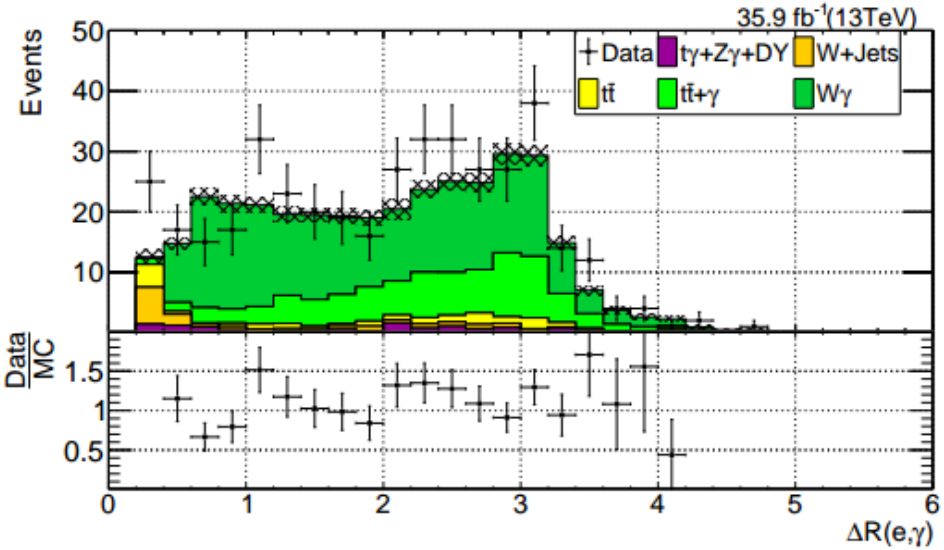

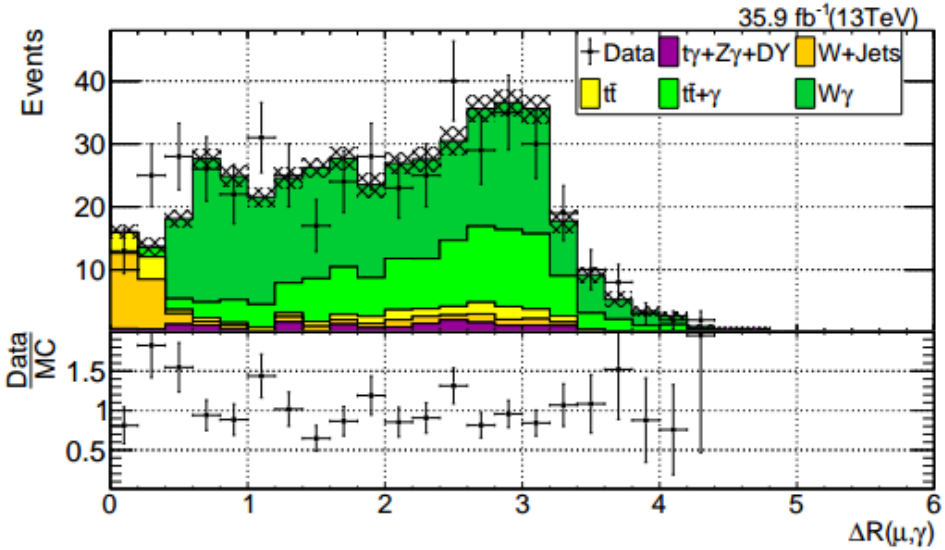

FIGURE 3.13: Distribution of $\Delta R(\ell, \gamma)$ for single electron (left) and single muon (right) events.

e+γ control regions

For thesis: all plots

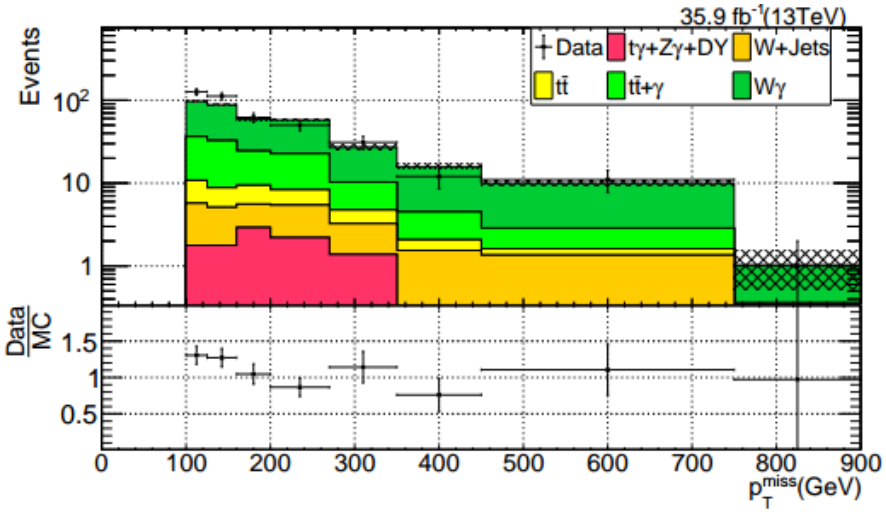

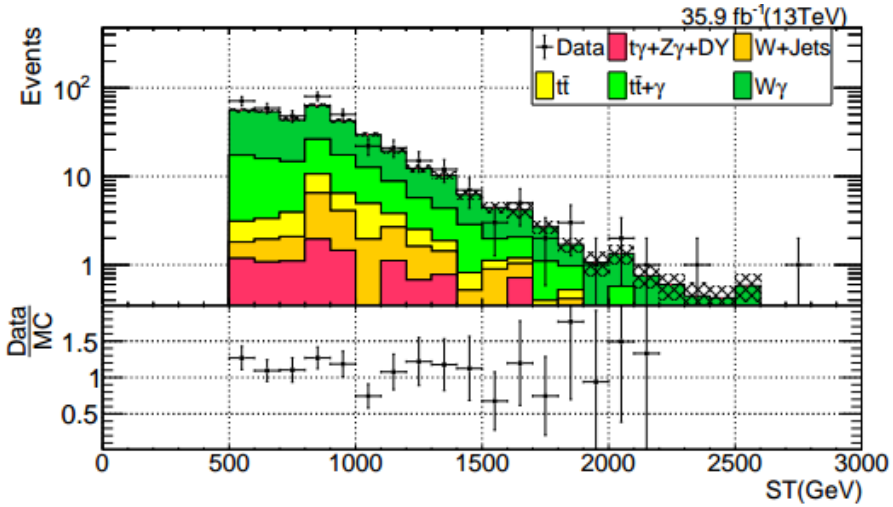

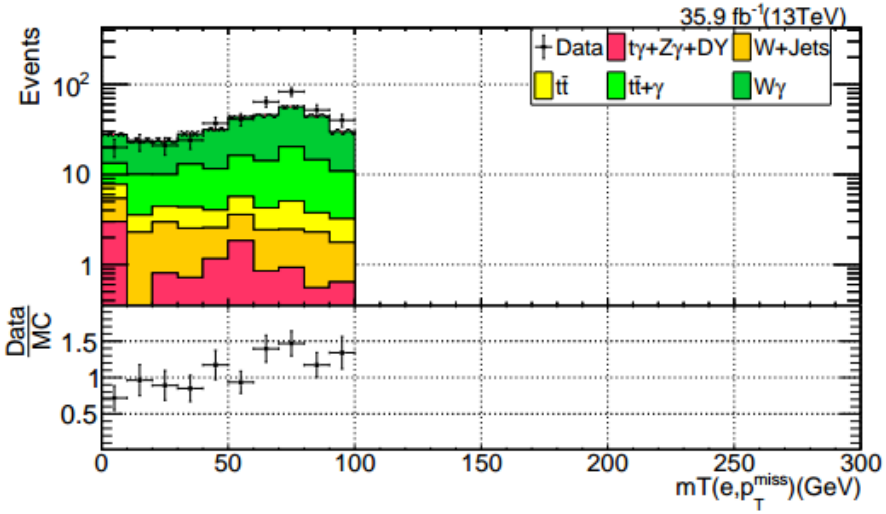

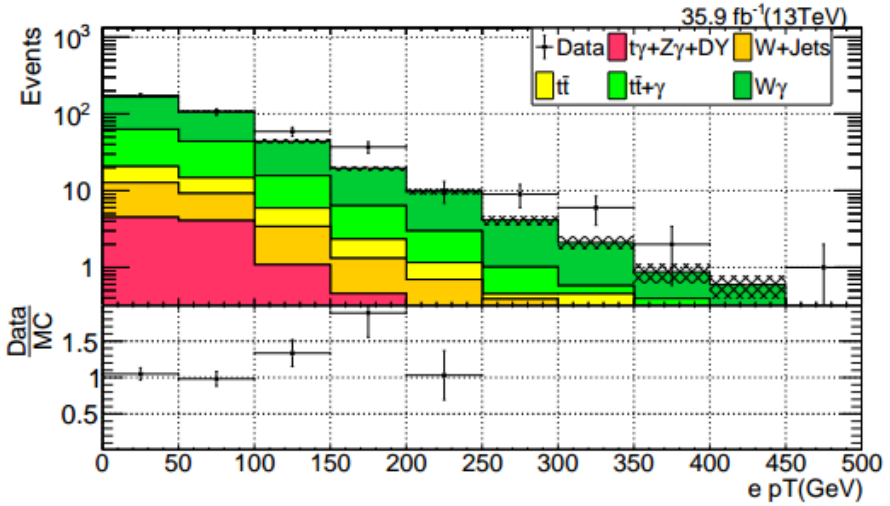

e+γ control regions

For thesis:
all plots

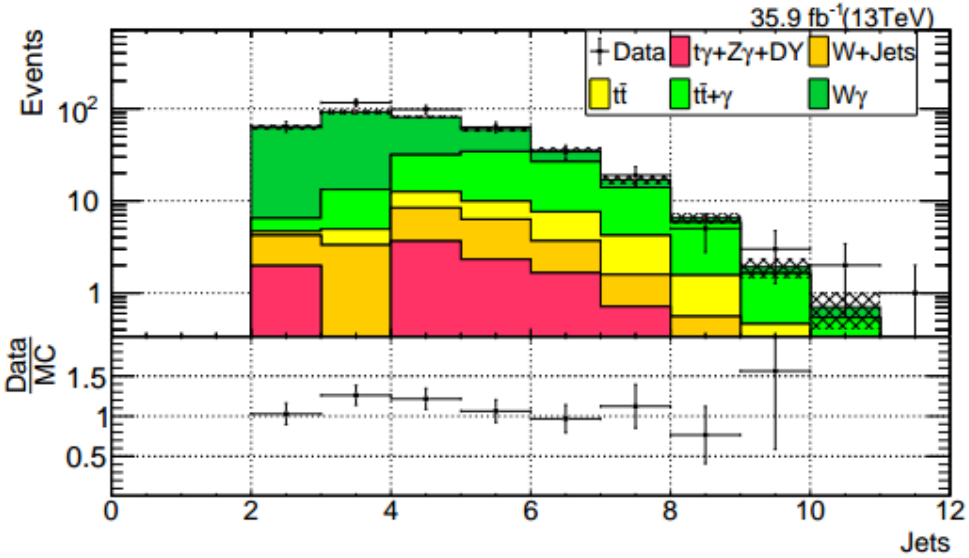

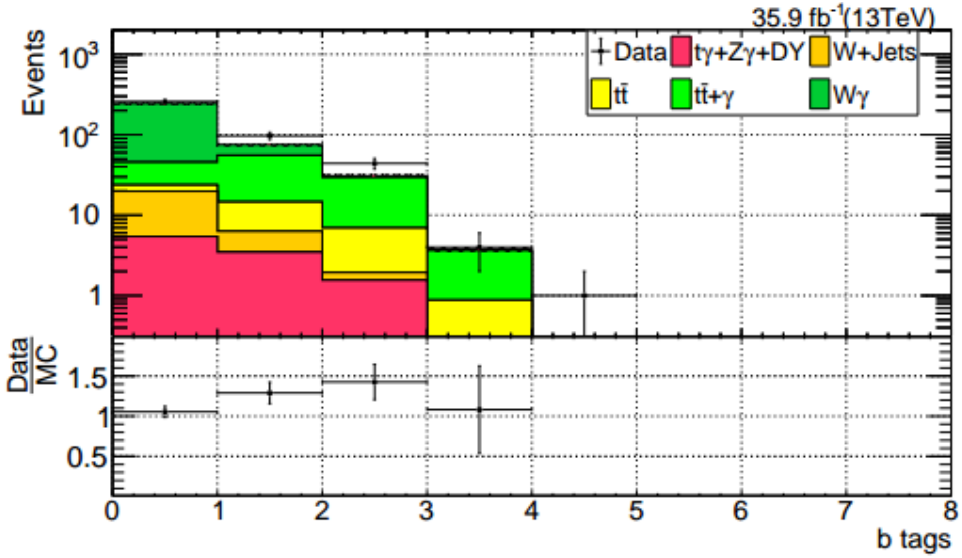

μ+γ control regions

For thesis: all plots

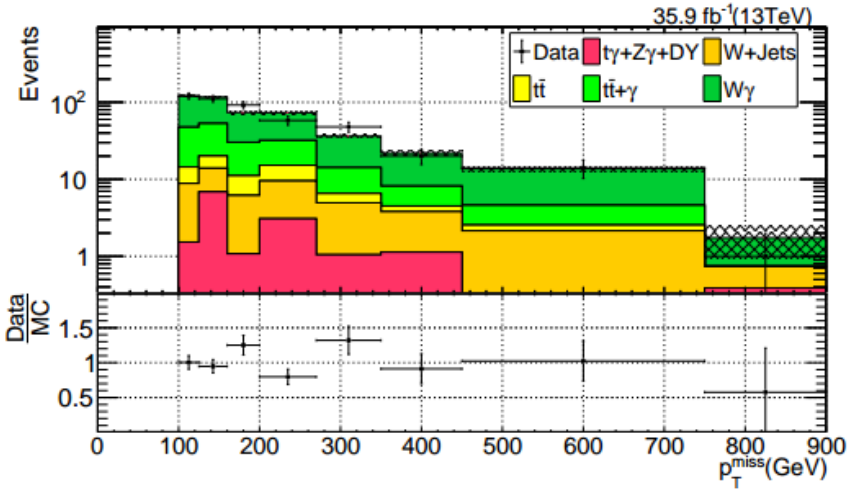

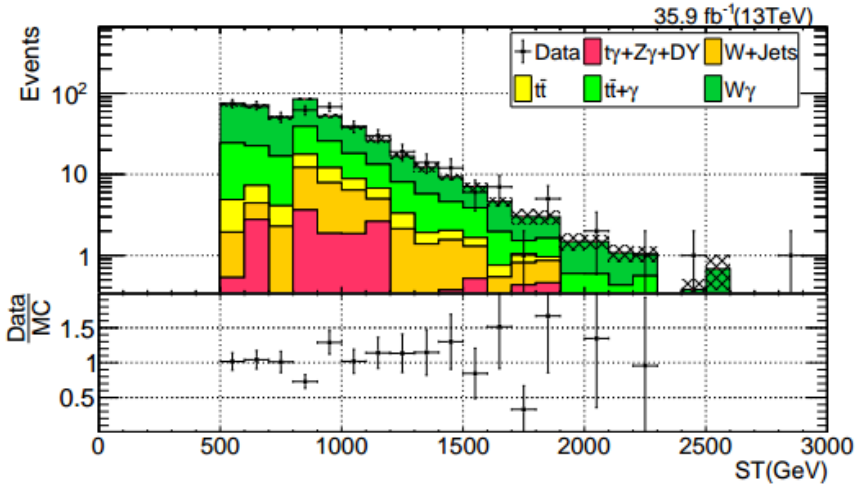

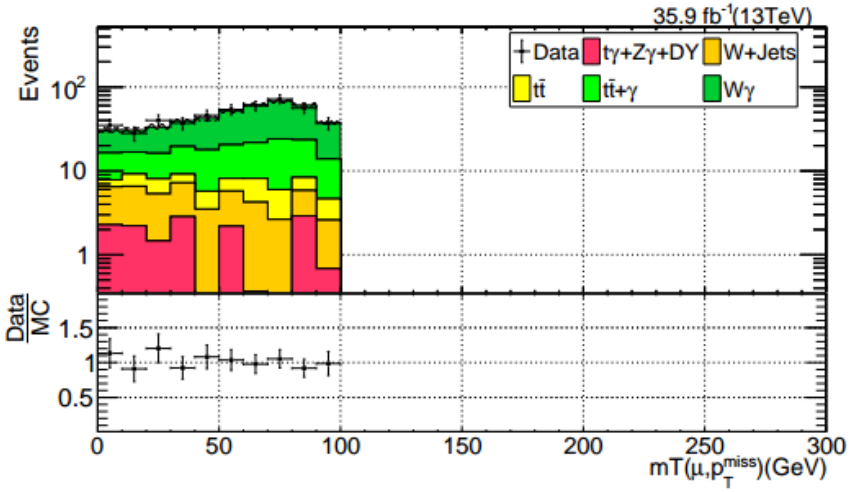

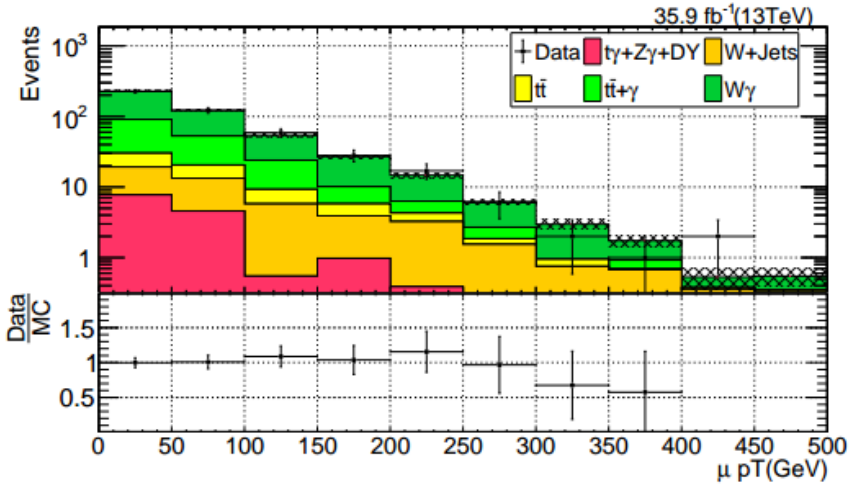

μ+γ control regions

For thesis:
all plots

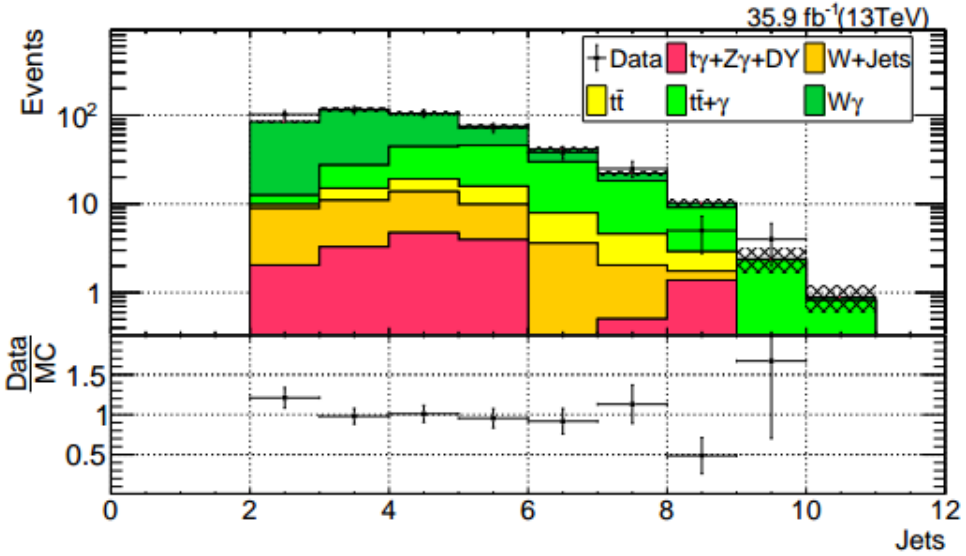

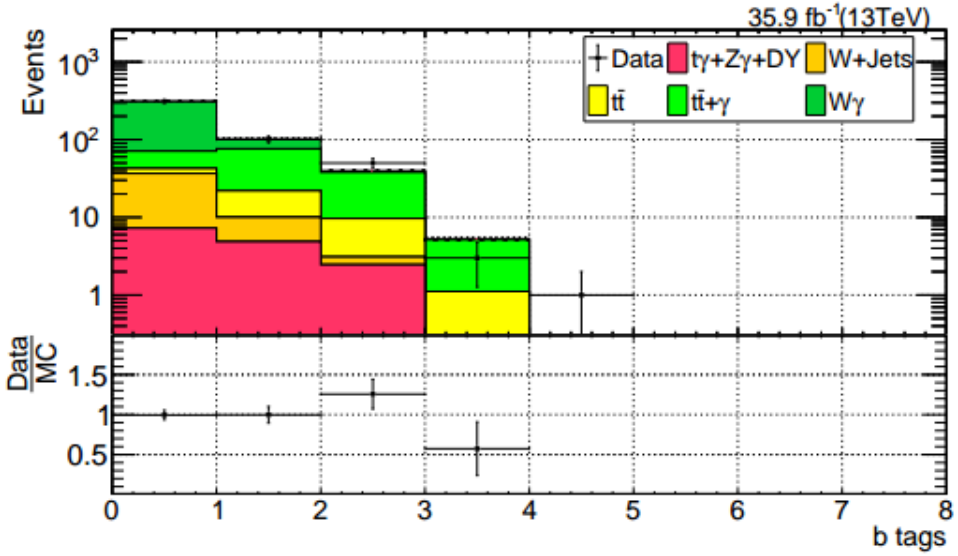

Estimation of e fake photon background

- The probability of electron faking photon is found to depend on the number of tracks near the electron.
- We study number of tracks (charge multiplicity, Qmult) in a jet matched to electron for various processes.

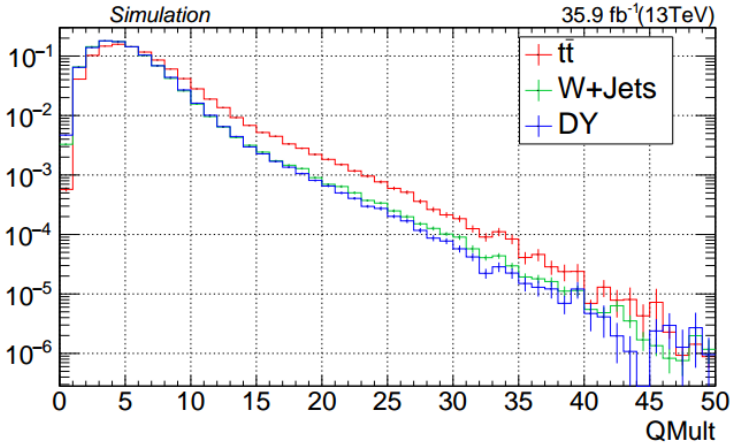

For thesis

FIGURE 3.14: Q_{mult} distribution in a jet matched to the electron in DY, W+jets, and $t\bar{t}$ events. Each of these distribution are scaled to unit area.

Fake rate closures in MC

For thesis:
3 plots

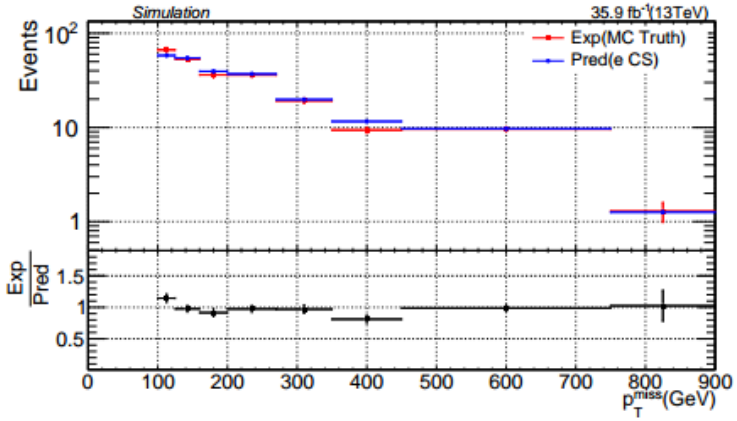

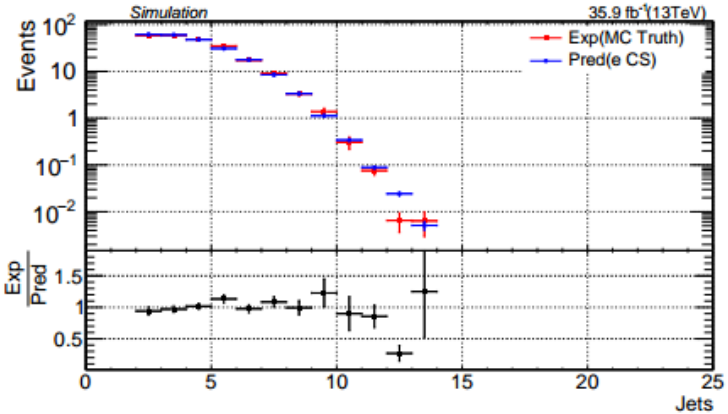

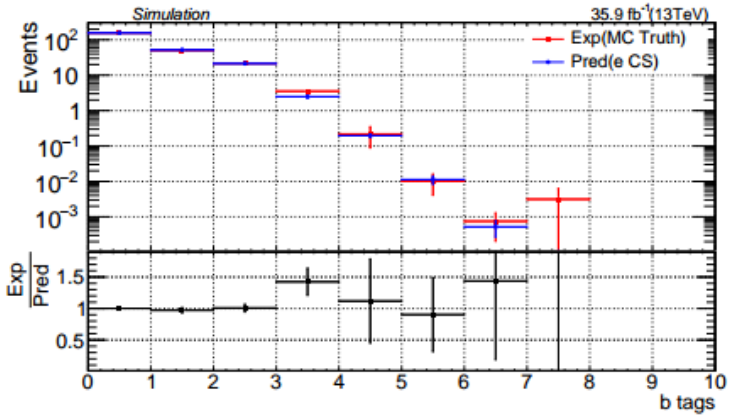

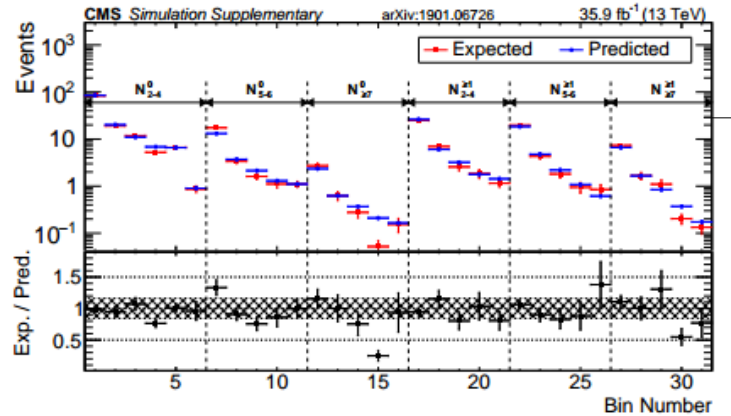

Already public

FIGURE 3.15: Comparison of fake rate prediction using fake rate parameterization and true MC yields using $W/t\bar{t}+(\gamma)$ simulations versus p_T^{miss} (top left), N_{jets} (top right), $N_{\text{b-jets}}$ (bottom left) and search bins (bottom right). The hashed region in the lower panel of bottom right plot shows the total systematic uncertainty.

Tag & probe fits – fake rate SFs

For thesis: all plots

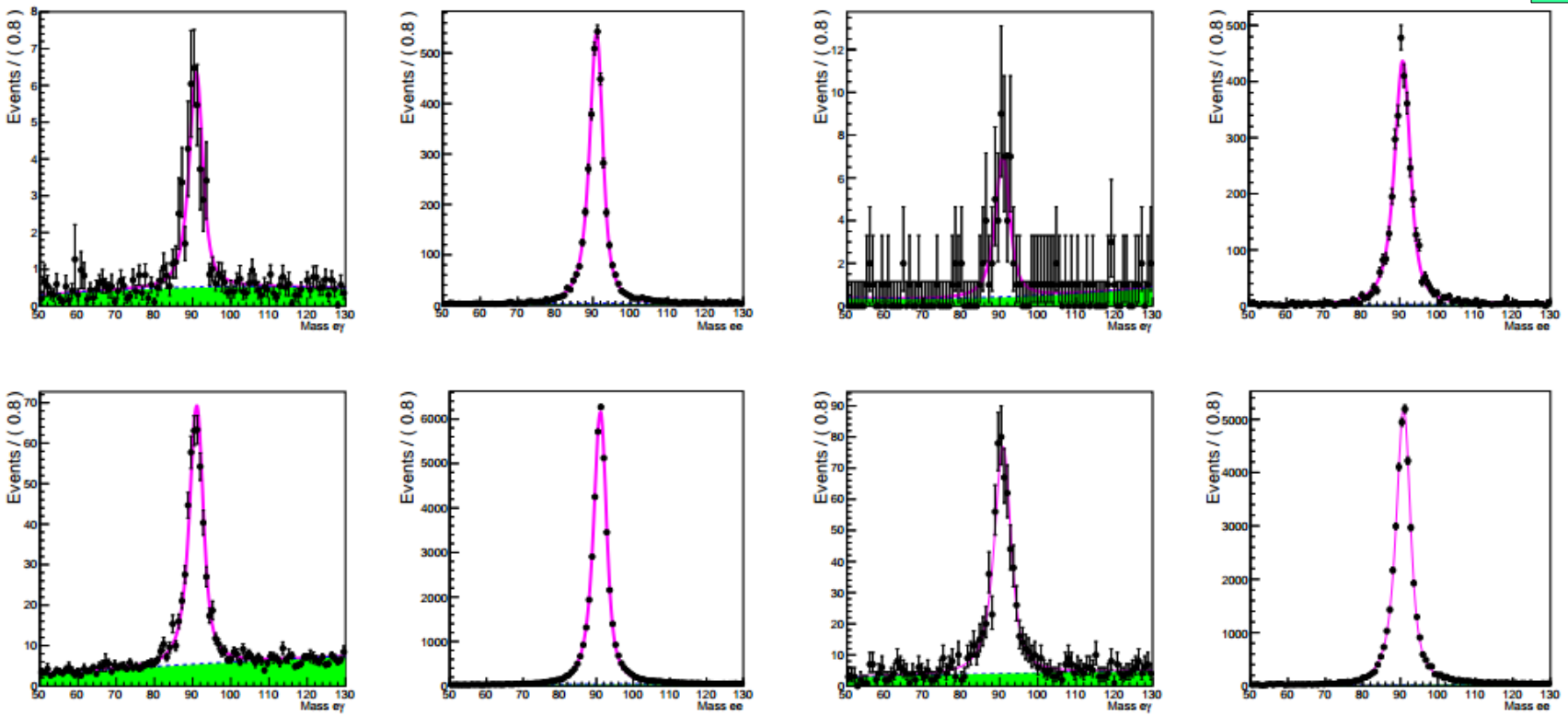

FIGURE 3.16: Tag & probe fits of the fake rate in 0-1 Q_{mult} bins (top row) and $\geq$ 2 Q_{mult} bins (bottom row). The first and second columns are the the photon region and electron region fits in MC, respectively. The third and fourth columns are the photon region and electron region fits in data, respectively.

Invisible Z background – llγ vs ννγ

For thesis: all plots

- Estimation of Z(νν)γ is done by taking Z(ll)γ yield in data for normalization and shape of MET, nJets and b-jets is taken from MC.
- The plots show that Z(ll)γ and Z(νν)γ are similar if the lepton pair is ignored.

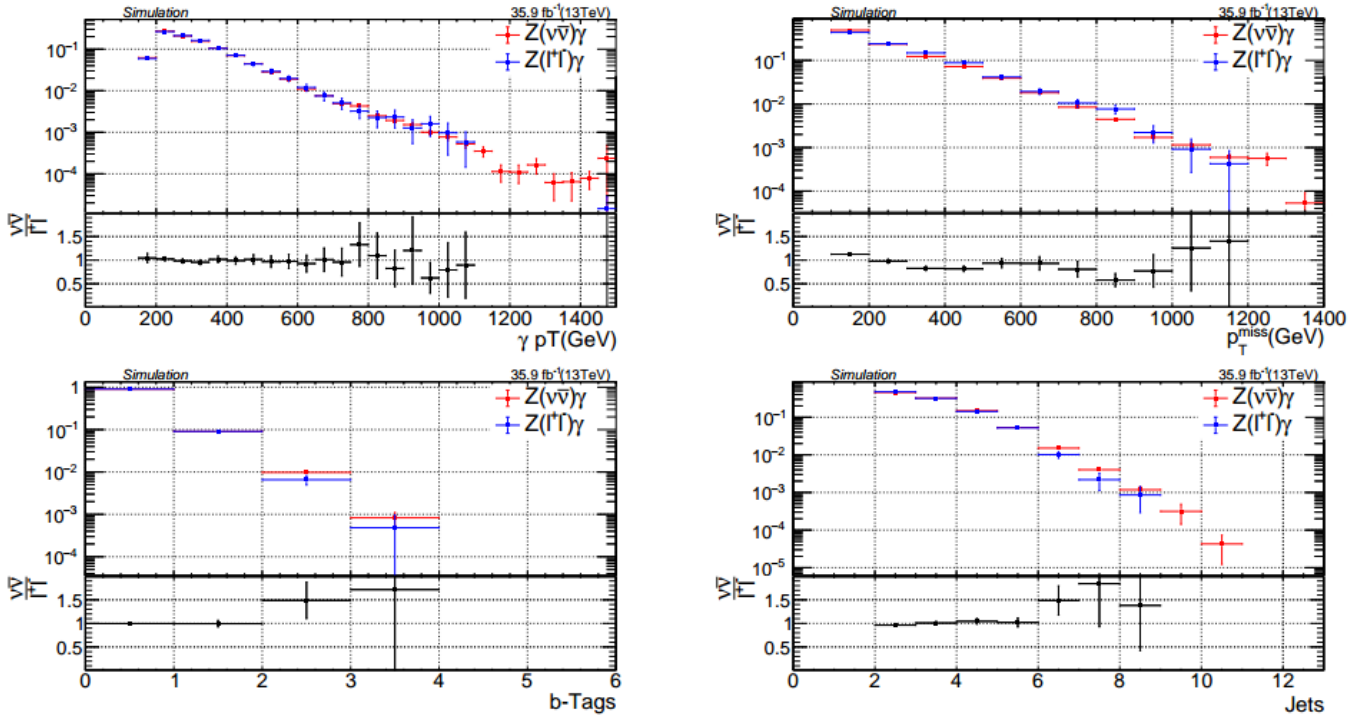

FIGURE 3.17: Comparison of $Z(ll)\gamma$ with $Z(\nu\nu)\gamma$ as function of p_T^γ (top left), p_T^{miss} (top right), $N_{\text{b-jets}}$ (bottom left) and N_{jets} (bottom right) for $p_T^\gamma > 190$ GeV

ll+γ control region

For thesis: all plots

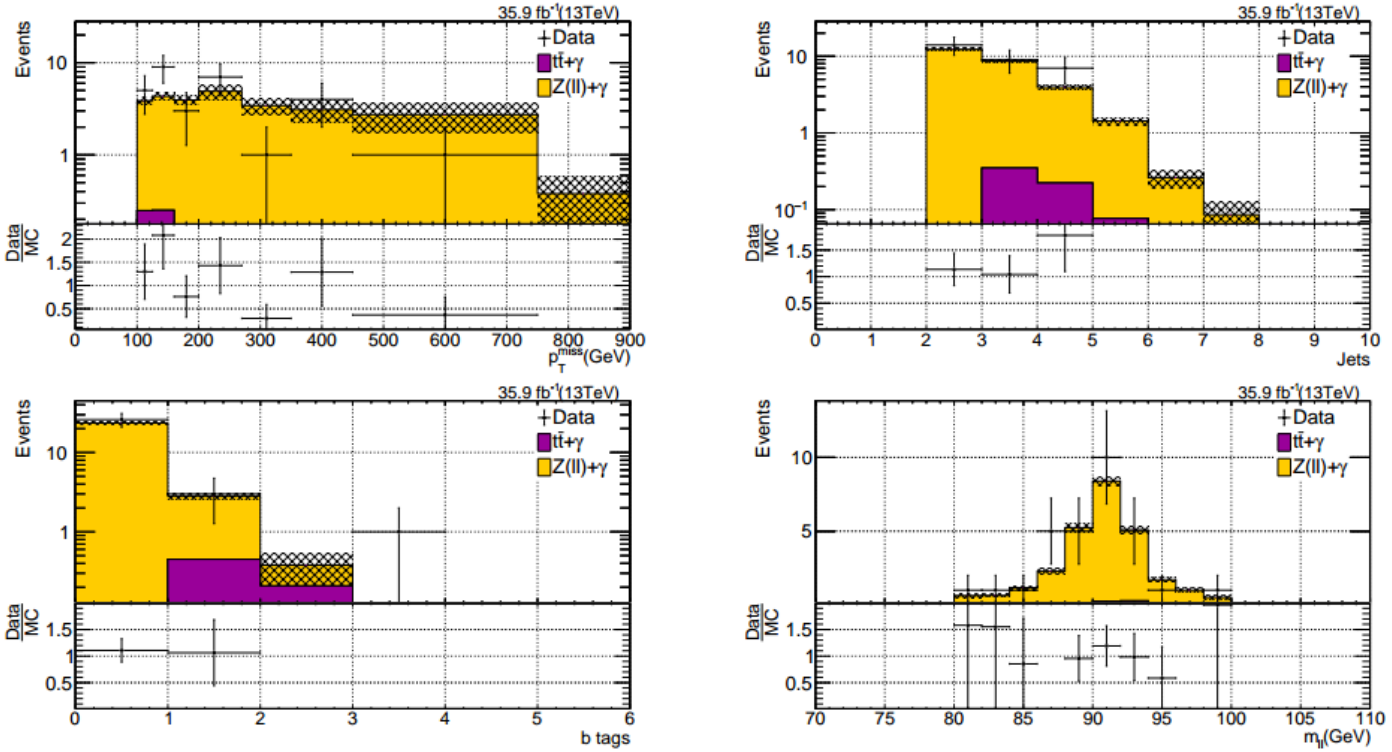

FIGURE B.3: Comparison of $ll + \gamma$ in data with $ll + \gamma$ events in MC as function of p_T^{miss} (top left), N_{jets} (top right), $N_{\text{b-jets}}$ (bottom left) and $m_{\ell\ell}$ (bottom right) for $p_T^{\gamma} > 190$GeV. Note that p_T^{miss} is calculated by ignoring the di-lepton pair. For the top left plot of p_T^{miss}, hashed error bars refer to statistical and EW correction uncertainties listed in Table 3.5. For the remaining 3 plots, error bars are statistical only.

γ + jets and QCD multijet estimation

- Use ABCD method by making use of low ΔΦ and low p_T^{miss} regions to predict this BG.
- p_T^{miss} and min($\Delta\Phi_1$, $\Delta\Phi_2$) are not completely independent.
- Take care of this dependence by applying a correction factor, K (double ratio), taken from MC simulation.

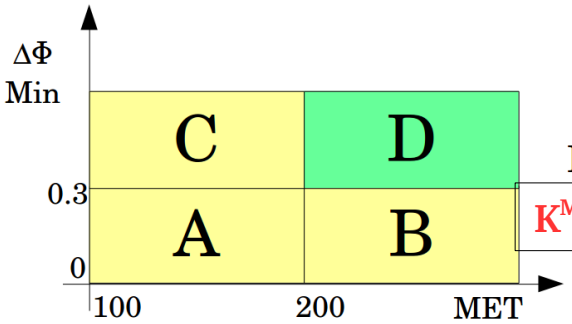

D = (C/A) * B * K

K^{MC}: (D/B)/(C/A)

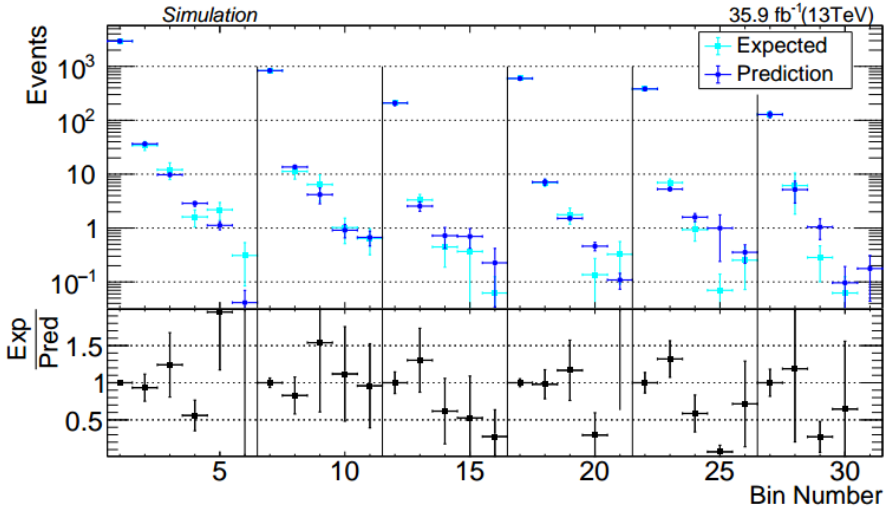

For thesis

FIGURE 3.20: Comparison of γ + jets and QCD multijet background estimated using low-$\Delta\phi$ control regions taken from MC (blue) to that expected in search regions (cyan).

0 photon region – closure for ABCD

- We validate our method in high stat region which consists of 0 photon events.
- This plot shows the MC closure using 0 photon events using the ABCD method.

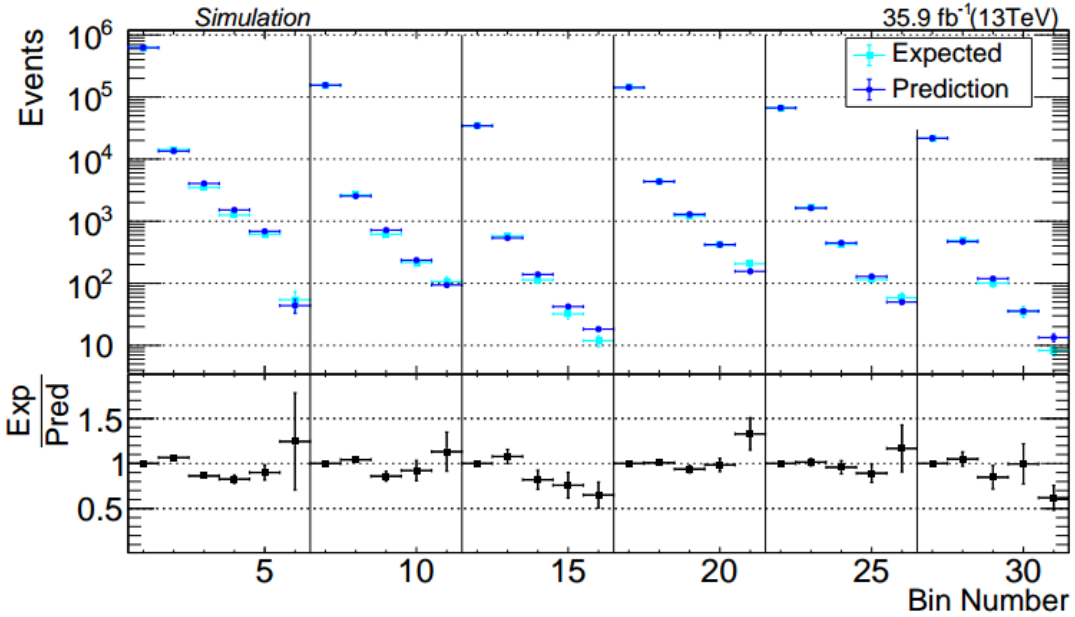

For thesis

FIGURE 3.21: In zero photon validation region in MC, comparison of γ + jets and QCD multijet background estimated using low-$\Delta\phi$ control regions taken from MC (blue) to that expected in search regions (cyan).

Signal acceptance × efficiency

For thesis: all plots

- For the models considered in the search (T5qqqqHG, T5bbbbZG, T5ttttZG and T6ttZG) plot acceptance x efficiency after applying all the event selections.

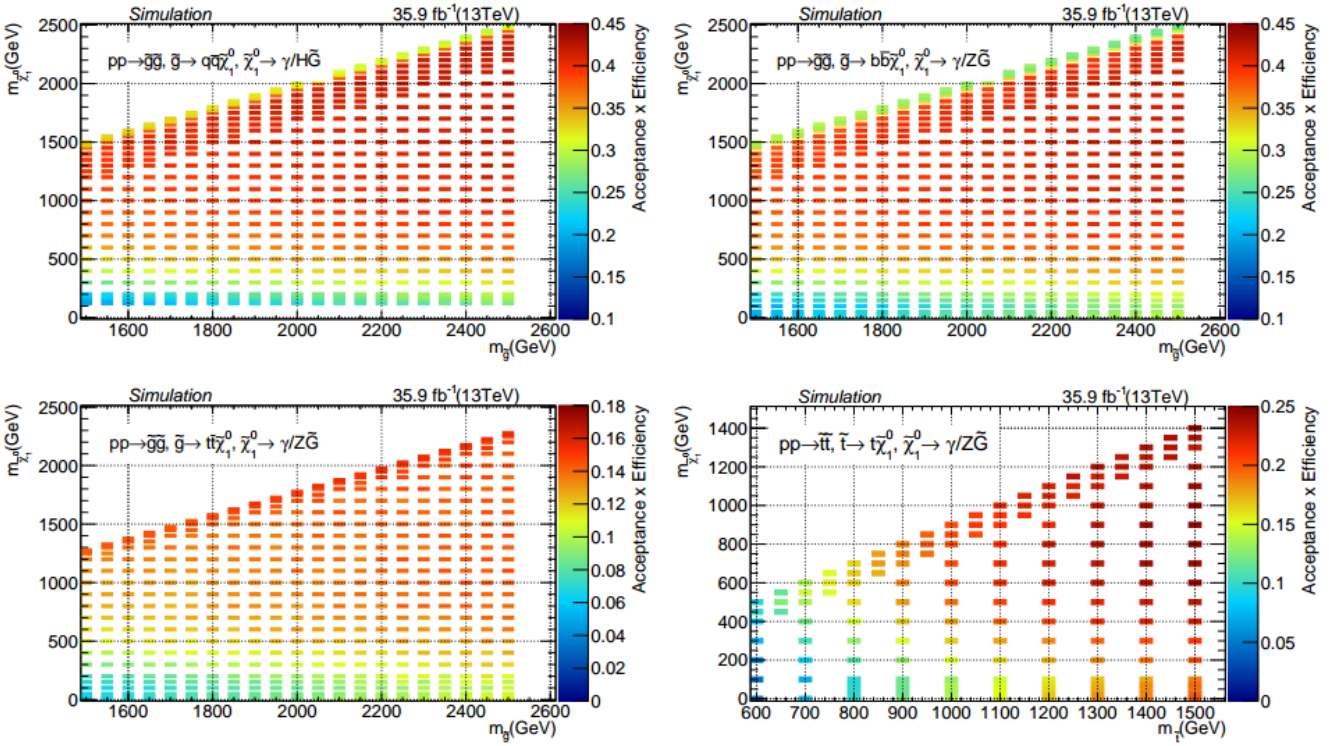

FIGURE B.4: Acceptance × efficiency for different mass points corresponding to T5qqqqHG (top left), T5bbbbZG (top right), T5ttttZG (bottom left) and T6ttZG (bottom right).

Expected exclusion limits for EW models

- We had studied sensitivity of the search for EW models.
- These plots show expected upper limit on cross section for two different EW models.

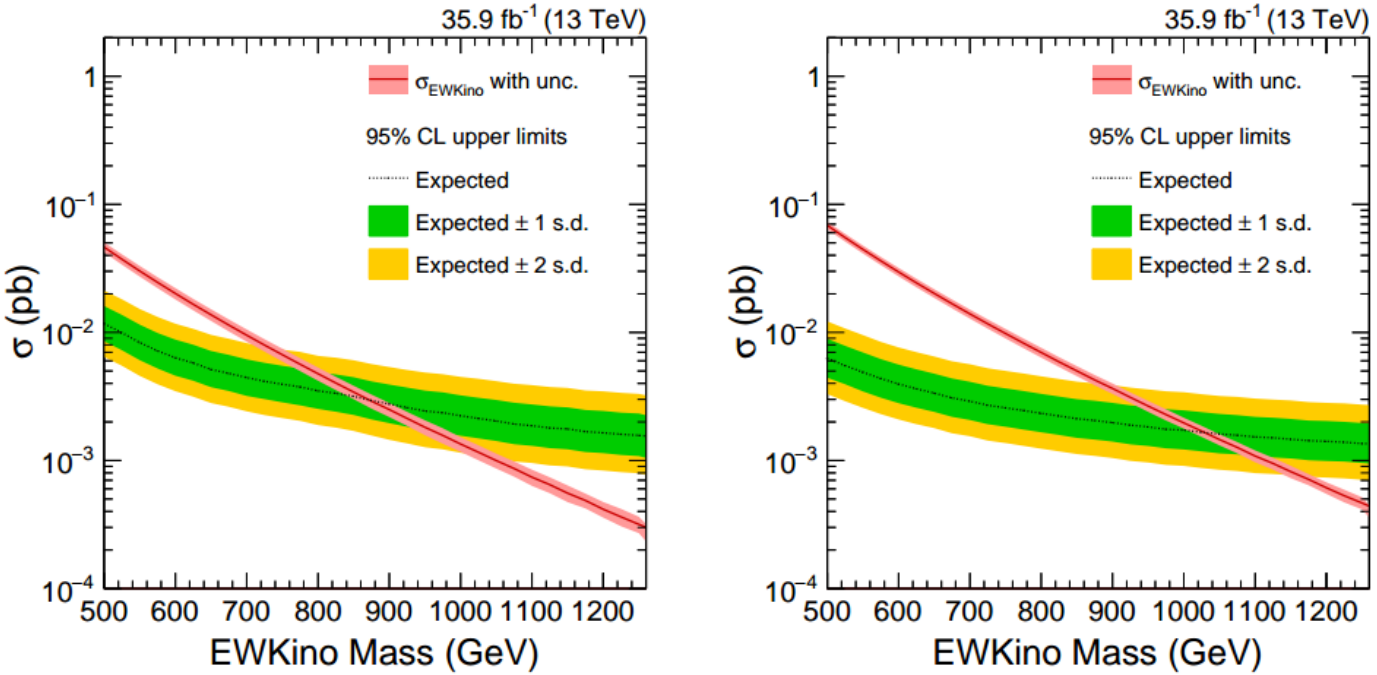

FIGURE 4.4: Expected upper limit on the cross section of TChiWG (left) and TChiNG (right) models.

For thesis: all plots

Data cleaning

- We had observed excess of events because of ECAL slew-rate effect in 2016 data. To mitigate this effect, following criteria was used: pT of the jet matched to photon > pT of the photon.

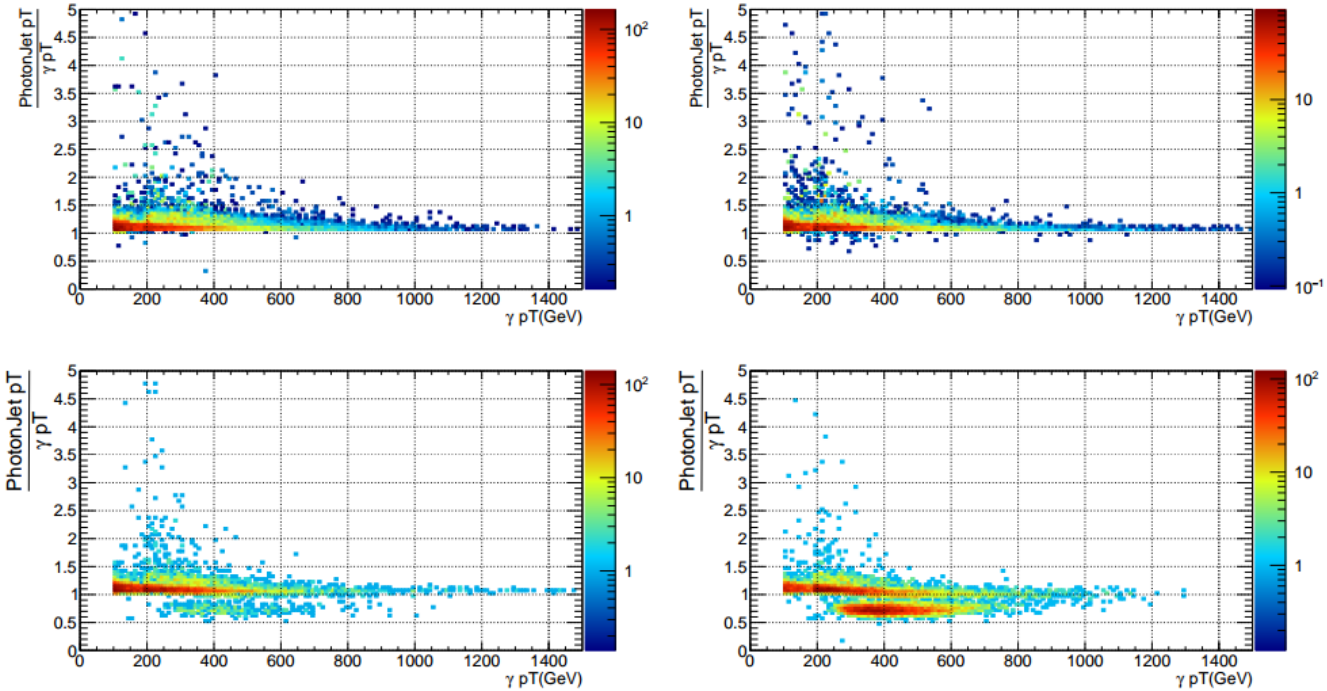

FIGURE C.1: Left column: $p_{\mathrm{T}}^{jet}/p_{\mathrm{T}}^{\gamma}$ as a function of p_{T}^{γ} in low-$\Delta\phi$ region with $p_T^{miss} > 100$ GeV region for events in γ + jets events in MC (top-left) and for data (bottom-left). Right column: same quantities in high-$\Delta\phi$ region with $100 < p_T^{miss} < 200$ GeV for γ + jets events in MC (top-right) and for data (bottom-right).

For thesis: all plots

Electron SF for MiniIso

- Derived SFs for various ID/Iso used by SUSY group, since I was EGM object contact for SUSY group.
- In our SUSY search, we used electrons with veto ID and miniIso < 0.1.
- The SFs were derived using standard EGM tools. I would like to add a these plots to explain how the Sfs are derived.

For thesis: all plots

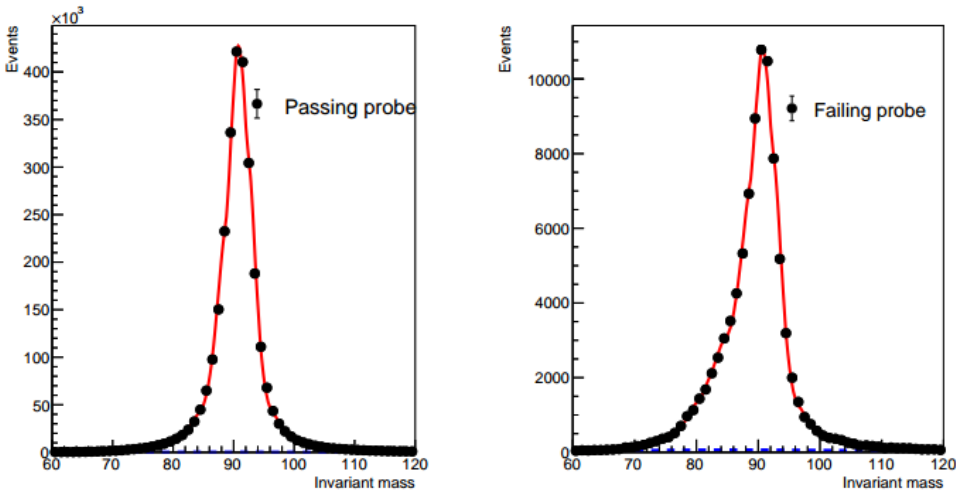

FIGURE 3.57: The left (right) plot shows the invariant mass distribution of tag and probe passing (failing) mini-isolation criteria.

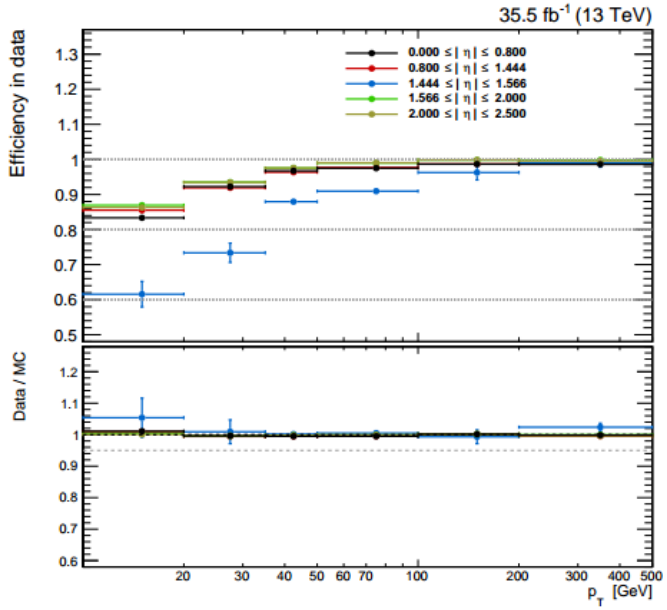

FIGURE 3.58: The efficiency of mini-isolation in data (top panel) as a function of electron p_T for various η regions and the bottom panel shows the SFs. The error bars include systematic and statistical uncertainties.

Additional tables

For thesis

Lost lepton + τ_{had} predictions

TABLE A.1: Observed events yields, average transfer factors (TFs) and predictions for lost-e and lost-μ + τ_{had} backgrounds in high $\Delta\phi$ regions.

Bin	Lost-e			Lost-μ		
	Obs.	Avg. TF	Pred.	Obs.	Avg. TF	Pred.
1	160	0.44 ± 0.07	70 ± 13	167	0.95 ± 0.07	159 ± 17
2	27	0.39 ± 0.06	10.5 ± 2.6	31	1.01 ± 0.07	31.2 ± 6.0
3	14	0.41 ± 0.07	5.8 ± 1.8	29	1.02 ± 0.07	29.6 ± 5.9
4	4	0.42 ± 0.07	1.68 ± 0.88	14	1.00 ± 0.07	13.9 ± 3.9
5	5	0.40 ± 0.06	1.98 ± 0.94	7	1.15 ± 0.08	8.1 ± 3.1
6	0	0.38 ± 0.06	$0.00^{+0.69}_{-0.00}$	1	1.23 ± 0.09	1.2 ± 1.2
7	23	0.28 ± 0.05	6.5 ± 1.8	31	0.66 ± 0.06	20.5 ± 4.1
8	5	0.26 ± 0.04	1.28 ± 0.61	8	0.64 ± 0.05	5.1 ± 1.9
9	8	0.26 ± 0.04	2.06 ± 0.80	5	0.64 ± 0.05	3.2 ± 1.5
10	3	0.26 ± 0.04	0.77 ± 0.46	1	0.64 ± 0.05	$0.64^{+0.65}_{-0.64}$
11	1	0.26 ± 0.04	0.26 ± 0.26	3	0.64 ± 0.05	1.9 ± 1.1
12	7	0.31 ± 0.08	2.2 ± 1.0	10	0.69 ± 0.10	6.9 ± 2.4
13	0	0.34 ± 0.09	$0.0^{+0.61}_{-0.0}$	0	0.73 ± 0.10	$0.0^{+1.3}_{-0.0}$
14	1	0.34 ± 0.09	$0.34^{+0.35}_{-0.34}$	2	0.73 ± 0.10	1.5 ± 1.0
15	1	0.34 ± 0.09	$0.34^{+0.35}_{-0.34}$	1	0.73 ± 0.10	0.73 ± 0.73
16	0	0.34 ± 0.09	$00.0^{+0.61}_{-0.00}$	0	0.73 ± 0.10	$0.0^{+1.3}_{-0.0}$
17	53	0.53 ± 0.09	28.2 ± 5.6	49	0.96 ± 0.10	47.2 ± 8.3
18	6	0.57 ± 0.09	3.4 ± 1.5	13	1.11 ± 0.11	14.5 ± 4.2
19	5	0.57 ± 0.09	2.9 ± 1.4	5	1.11 ± 0.11	5.6 ± 2.5
20	0	0.57 ± 0.09	$0.0^{+1.0}_{-0.0}$	1	1.11 ± 0.11	1.1 ± 1.1
21	4	0.57 ± 0.09	2.3 ± 1.2	4	1.11 ± 0.11	4.4 ± 2.3
22	41	0.39 ± 0.07	15.9 ± 3.7	51	0.73 ± 0.08	37.4 ± 6.5
23	10	0.35 ± 0.06	3.5 ± 1.3	3	0.79 ± 0.08	2.4 ± 1.4
24	3	0.35 ± 0.06	1.06 ± 0.64	5	0.79 ± 0.08	4.0 ± 1.8
25	2	0.35 ± 0.06	0.71 ± 0.51	3	0.79 ± 0.08	2.4 ± 1.4
26	1	0.35 ± 0.06	$0.35^{+0.36}_{-0.35}$	0	0.79 ± 0.08	$0.0^{+1.43}_{-0.0}$
27	16	0.43 ± 0.10	6.9 ± 2.3	16	0.65 ± 0.10	10.4 ± 3.0
28	2	0.36 ± 0.08	0.72 ± 0.53	3	0.66 ± 0.10	2.0 ± 1.2
29	0	0.36 ± 0.08	$0.00^{+0.65}_{-0.00}$	2	0.66 ± 0.10	1.33 ± 0.96
30	2	0.36 ± 0.08	0.72 ± 0.53	0	0.66 ± 0.10	$0.0^{+1.2}_{-0.0}$
31	1	0.36 ± 0.08	$0.36^{+0.37}_{-0.36}$	0	0.66 ± 0.10	$0.0^{+1.2}_{-0.0}$

TABLE A.2: Observed events yields, average transfer factors (TFs) and predictions for lost-e and lost-μ + τ_{had} backgrounds in the low-$\Delta\Phi$ control region.

Bin	Lost-e			Lost-μ		
	Obs.	Avg. TF	Pred.	Obs.	Avg. TF	Pred.
1	77	0.20 ± 0.04	15.5 ± 3.9	62	0.64 ± 0.09	39.5 ± 7.7
2	22	0.16 ± 0.04	3.6 ± 1.1	25	0.57 ± 0.06	14.2 ± 3.3
3	11	0.18 ± 0.04	1.93 ± 0.74	7	0.63 ± 0.07	4.4 ± 1.7
4	6	0.16 ± 0.04	0.94 ± 0.44	5	0.66 ± 0.07	3.3 ± 1.5
5	7	0.17 ± 0.04	1.22 ± 0.55	11	0.59 ± 0.07	6.4 ± 2.1
6	0	0.17 ± 0.04	$0.00^{+0.31}_{-0.00}$	0	0.58 ± 0.07	$0.0^{+1.1}_{-0.0}$
7	10	0.19 ± 0.04	1.95 ± 0.76	13	0.54 ± 0.11	7.1 ± 2.4
8	1	0.17 ± 0.04	0.17 ± 0.17	1	0.54 ± 0.07	$0.54^{+0.55}_{-0.54}$
9	2	0.17 ± 0.04	0.33 ± 0.25	3	0.54 ± 0.07	1.63 ± 0.96
10	2	0.17 ± 0.04	0.33 ± 0.25	1	0.54 ± 0.07	$0.54^{+0.55}_{-0.54}$
11	0	0.17 ± 0.04	$0.00^{+0.30}_{-0.00}$	1	0.54 ± 0.07	$0.54^{+0.55}_{-0.54}$
12	1	0.26 ± 0.09	$0.26^{+0.28}_{-0.26}$	4	0.43 ± 0.12	1.72 ± 0.99
13	1	0.17 ± 0.06	$0.17^{+0.18}_{-0.17}$	2	0.59 ± 0.20	1.19 ± 0.93
14	0	0.17 ± 0.06	$0.00^{+0.31}_{-0.00}$	0	0.59 ± 0.20	$0.0^{+1.1}_{-0.0}$
15	1	0.17 ± 0.06	$0.17^{+0.18}_{-0.17}$	1	0.59 ± 0.20	$0.59^{+0.63}_{-0.59}$
16	0	0.17 ± 0.06	$0.00^{+0.31}_{-0.00}$	1	0.59 ± 0.20	$0.59^{+0.63}_{-0.59}$
17	26	0.39 ± 0.08	10.2 ± 2.9	22	0.86 ± 0.16	18.8 ± 5.3
18	4	0.27 ± 0.06	1.10 ± 0.59	4	0.68 ± 0.10	2.7 ± 1.4
19	1	0.27 ± 0.06	$0.27^{+0.28}_{-0.27}$	2	0.68 ± 0.10	1.37 ± 0.99
20	2	0.27 ± 0.06	0.55 ± 0.40	0	0.68 ± 0.10	$0.0^{+1.2}_{-0.0}$
21	0	0.27 ± 0.06	$0.00^{+0.49}_{-0.00}$	2	0.68 ± 0.10	1.37 ± 0.99
22	9	0.23 ± 0.06	2.03 ± 0.87	14	0.73 ± 0.13	10.2 ± 3.3
23	5	0.25 ± 0.06	1.26 ± 0.63	2	0.54 ± 0.08	1.07 ± 0.77
24	1	0.25 ± 0.06	$0.25^{+0.26}_{-0.25}$	1	0.54 ± 0.08	0.54 ± 0.54
25	1	0.25 ± 0.06	$0.25^{+0.26}_{-0.25}$	1	0.54 ± 0.08	0.54 ± 0.54
26	2	0.25 ± 0.06	0.50 ± 0.37	1	0.54 ± 0.08	0.54 ± 0.54
27	3	0.27 ± 0.10	0.81 ± 0.56	4	0.51 ± 0.12	2.0 ± 1.1
28	2	0.25 ± 0.07	0.50 ± 0.38	3	0.53 ± 0.10	1.59 ± 0.97
29	1	0.25 ± 0.07	$0.25^{+0.26}_{-0.25}$	0	0.53 ± 0.10	$0.00^{+0.95}_{-0.00}$
30	1	0.25 ± 0.07	$0.25^{+0.26}_{-0.25}$	0	0.53 ± 0.10	$0.00^{+0.95}_{-0.00}$
31	0	0.25 ± 0.07	$0.00^{+0.45}_{-0.00}$	0	0.53 ± 0.10	$0.00^{+0.95}_{-0.00}$

For thesis

Electron fake photon

TABLE A.3: Fake rate parameterization derived from W/$t\bar{t}$ simulations.

p_T	Q_{mult}	fake rate
100 – 120	0 – 1	0.0261 ± 0.0029
	2 – 4	0.0125 ± 0.0009
	4 – 7	0.0080 ± 0.0006
	≥ 7	0.0052 ± 0.0006
120 – 140	0 – 1	0.0208 ± 0.0028
	2 – 4	0.0118 ± 0.0011
	4 – 7	0.0068 ± 0.0006
	≥ 7	0.0050 ± 0.0006
140 – 160	0 – 1	0.0263 ± 0.0036
	2 – 4	0.0094 ± 0.0010
	4 – 7	0.0079 ± 0.0007
	≥ 7	0.0028 ± 0.0004
160 – 180	0 – 1	0.0243 ± 0.0041
	2 – 4	0.0114 ± 0.0012
	4 – 7	0.0065 ± 0.0007
	≥ 7	0.0034 ± 0.0006
180 – 200	0 – 1	0.0194 ± 0.0038
	2 – 4	0.0070 ± 0.0011
	4 – 7	0.0070 ± 0.0009
	≥ 7	0.0040 ± 0.0008
200 – 230	0 – 1	0.0177 ± 0.0030
	2 – 4	0.0104 ± 0.0014
	4 – 7	0.0044 ± 0.0005
	≥ 7	0.0042 ± 0.0008
230 – 260	0 – 1	0.0235 ± 0.0052
	2 – 4	0.0062 ± 0.0011
	4 – 7	0.0051 ± 0.0008
	≥ 7	0.0034 ± 0.0007
260 – 300	0 – 1	0.0293 ± 0.0079
	2 – 4	0.0096 ± 0.0014
	4 – 7	0.0062 ± 0.0010
	≥ 7	0.0075 ± 0.0017
300 – 380	0 – 1	0.0224 ± 0.0052
	2 – 4	0.0091 ± 0.0014
	4 – 7	0.0073 ± 0.0009
	≥ 7	0.0035 ± 0.0006
380 – 500	0 – 1	0.0232 ± 0.0048
	2 – 4	0.0084 ± 0.0011
	4 – 7	0.0047 ± 0.0006
	≥ 7	0.0036 ± 0.0008
> 500	0 – 1	0.0210 ± 0.0041
	2 – 4	0.0102 ± 0.0015
	4 – 7	0.0076 ± 0.0010
	≥ 7	0.0047 ± 0.0014

For thesis

TABLE A.4: Observed single electron yields, after accounting for lepton scale factors and relative trigger efficiencies factor, in each of the signal regions, the average scale factor due to MC-based fake rates and data/MC fake rate correction factors from T&P measurements, and the corresponding fake-rate predictions with all the uncertainties (statistical and systematic) taken into consideration.

Bin	Obs. e events	Avg. transfer factor	Prediction
1	11777	0.0089 ± 0.0022	105 ± 25
2	2426	0.0092 ± 0.0022	22.3 ± 5.4
3	1259	0.0094 ± 0.0023	11.9 ± 2.9
4	699	0.0094 ± 0.0022	6.6 ± 1.6
5	668	0.0100 ± 0.0022	6.7 ± 1.5
6	77	0.0103 ± 0.0021	0.79 ± 0.19
7	1551	0.0090 ± 0.0020	13.9 ± 3.2
8	410	0.0086 ± 0.0018	3.53 ± 0.75
9	249	0.0096 ± 0.0022	2.39 ± 0.56
10	136	0.0092 ± 0.0020	1.26 ± 0.30
11	104	0.0096 ± 0.0021	1.00 ± 0.24
12	255	0.0087 ± 0.0018	2.21 ± 0.47
13	75	0.0095 ± 0.0019	0.72 ± 0.16
14	44	0.0086 ± 0.0019	0.38 ± 0.10
15	20	0.0084 ± 0.0016	0.17 ± 0.05
16	17	0.0117 ± 0.0024	0.20 ± 0.06
17	3879	0.0084 ± 0.0019	32.4 ± 7.5
18	861	0.0083 ± 0.0019	7.1 ± 1.7
19	435	0.0087 ± 0.0021	3.79 ± 0.92
20	232	0.0086 ± 0.0019	2.00 ± 0.45
21	172	0.0094 ± 0.0021	1.62 ± 0.38
22	2322	0.0085 ± 0.0018	19.8 ± 4.3
23	635	0.0087 ± 0.0019	5.5 ± 1.2
24	331	0.0090 ± 0.0018	2.98 ± 0.63
25	169	0.0082 ± 0.0016	1.38 ± 0.30
26	80	0.0083 ± 0.0016	0.67 ± 0.15
27	740	0.0087 ± 0.0017	6.4 ± 1.3
28	184	0.0092 ± 0.0019	1.68 ± 0.37
29	98	0.0075 ± 0.0014	0.73 ± 0.16
30	57	0.0076 ± 0.0015	0.44 ± 0.10
31	26	0.0089 ± 0.0018	0.23 ± 0.07

TABLE A.5: Observed single electron yields, after accounting for lepton scale factors and relative trigger efficiencies factor, in each of the low-$\Delta\phi$ control regions, the average scale factor due to MC-based fake rates and data/MC fake rate correction factors from T&P measurements, and the corresponding fake-rate predictions with all the uncertainties (statistical and systematic) taken into consideration.

Bin	Obs. e events	Avg. transfer factor	Prediction
1	994	0.0122 ± 0.0050	12.2 ± 5.0
2	177	0.0127 ± 0.0049	2.24 ± 0.89
3	100	0.0117 ± 0.0044	1.17 ± 0.45
4	59	0.0140 ± 0.0059	0.82 ± 0.37
5	33	0.0127 ± 0.0050	0.42 ± 0.18
6	3	0.0154 ± 0.0053	0.05 ± 0.03
7	207	0.0116 ± 0.0041	2.41 ± 0.87
8	43	0.0112 ± 0.0040	0.48 ± 0.19
9	14	0.0071 ± 0.0023	0.10 ± 0.04
10	3	0.0179 ± 0.0048	0.05 ± 0.03
11	3	0.0222 ± 0.0097	0.07 ± 0.05
12	36	0.0106 ± 0.0036	0.38 ± 0.14
13	8	0.0080 ± 0.0022	0.06 ± 0.03
14	3	0.0075 ± 0.0029	0.02 ± 0.02
15	2	0.0185 ± 0.0053	0.04 ± 0.03
16	0	0.0222 ± 0.0097	0.00 ± 0.04
17	513	0.0115 ± 0.0043	5.9 ± 2.2
18	132	0.0120 ± 0.0044	1.58 ± 0.59
19	58	0.0100 ± 0.0037	0.58 ± 0.23
20	23	0.0133 ± 0.0043	0.31 ± 0.12
21	26	0.0106 ± 0.0041	0.28 ± 0.12
22	358	0.0112 ± 0.0040	4.0 ± 1.5
23	80	0.0110 ± 0.0037	0.88 ± 0.31
24	35	0.0092 ± 0.0030	0.32 ± 0.12
25	20	0.0102 ± 0.0029	0.20 ± 0.07
26	8	0.0089 ± 0.0054	0.07 ± 0.05
27	106	0.0117 ± 0.0039	1.24 ± 0.43
28	23	0.0110 ± 0.0030	0.25 ± 0.09
29	15	0.0115 ± 0.0048	0.17 ± 0.09
30	6	0.0115 ± 0.0028	0.07 ± 0.03
31	2	0.0073 ± 0.0018	0.01 ± 0.01

Electron fake photon predictions

For thesis

Invisible Z estimation

TABLE A.6: $Z(\nu\nu) + \gamma$ MC yields and prediction for the high $\Delta\phi$ regions.

Bin	MC Yield	Prediction
1	80.90 ± 0.68	92 ± 17
2	29.46 ± 0.41	33.6 ± 8.3
3	20.06 ± 0.34	22.9 ± 6.0
4	14.90 ± 0.29	17.0 ± 5.2
5	15.92 ± 0.30	18.1 ± 7.1
6	2.46 ± 0.12	2.8 ± 1.2
7	7.30 ± 0.23	8.3 ± 1.6
8	2.71 ± 0.14	3.09 ± 0.78
9	1.74 ± 0.12	1.98 ± 0.54
10	1.31 ± 0.10	1.49 ± 0.47
11	1.44 ± 0.11	1.65 ± 0.65
12	0.70 ± 0.08	0.80 ± 0.18
13	0.32 ± 0.06	0.37 ± 0.11
14	0.21 ± 0.05	0.24 ± 0.08
15	0.14 ± 0.04	0.16 ± 0.07
16	0.15 ± 0.03	0.17 ± 0.08
17	8.43 ± 0.14	9.6 ± 1.8
18	3.12 ± 0.08	3.55 ± 0.89
19	2.15 ± 0.07	2.45 ± 0.65
20	1.59 ± 0.05	1.81 ± 0.55
21	1.88 ± 0.06	2.14 ± 0.84
22	1.63 ± 0.08	1.86 ± 0.36
23	0.67 ± 0.06	0.76 ± 0.20
24	0.43 ± 0.04	0.49 ± 0.14
25	0.28 ± 0.03	0.32 ± 0.11
26	0.42 ± 0.06	0.48 ± 0.20
27	0.19 ± 0.02	0.21 ± 0.05
28	0.12 ± 0.02	0.13 ± 0.04
29	0.09 ± 0.03	0.10 ± 0.04
30	0.06 ± 0.02	0.07 ± 0.03
31	0.04 ± 0.01	0.04 ± 0.02

TABLE A.7: $Z(\nu\nu) + \gamma$ MC yields and prediction for the low $\Delta\phi$ regions.

Bin	MC Yield	Prediction
1	19.13 ± 0.32	21.3 ± 4.4
2	7.46 ± 0.22	8.3 ± 2.2
3	4.52 ± 0.17	5.0 ± 1.4
4	2.91 ± 0.14	3.2 ± 1.0
5	2.01 ± 0.12	2.24 ± 0.90
6	0.16 ± 0.03	0.18 ± 0.09
7	1.77 ± 0.14	1.97 ± 0.43
8	0.72 ± 0.09	0.80 ± 0.23
9	0.51 ± 0.08	0.57 ± 0.18
10	0.24 ± 0.05	0.26 ± 0.10
11	0.20 ± 0.04	0.23 ± 0.10
12	0.21 ± 0.05	0.23 ± 0.07
13	0.12 ± 0.04	0.14 ± 0.06
14	0.04 ± 0.01	0.04 ± 0.02
15	0.02 ± 0.01	0.03 ± 0.01
16	0.02 ± 0.01	0.03 ± 0.01
17	2.05 ± 0.07	2.28 ± 0.49
18	0.81 ± 0.05	0.90 ± 0.24
19	0.48 ± 0.03	0.53 ± 0.15
20	0.34 ± 0.03	0.38 ± 0.13
21	0.28 ± 0.04	0.31 ± 0.13
22	0.54 ± 0.08	0.60 ± 0.15
23	0.16 ± 0.03	0.17 ± 0.06
24	0.11 ± 0.03	0.12 ± 0.04
25	0.06 ± 0.01	0.06 ± 0.02
26	0.07 ± 0.02	0.08 ± 0.04
27	0.06 ± 0.01	0.06 ± 0.02
28	0.04 ± 0.02	0.04 ± 0.02
29	0.01 ± 0.01	0.02 ± 0.01
30	0.008 ± 0.003	0.009 ± 0.005
31	0.006 ± 0.003	0.007 ± 0.004

For thesis

TABLE A.8: Fake p_T^{miss} background control sample statistics and electroweak predictions with uncertainties.

$N_{jets}^{b\text{-jets}}$	Bin	Low $\Delta\phi$ raw	EW low $\Delta\phi$	γ + jets low $\Delta\phi$	γ + jets high $\Delta\phi$
N_{2-4}^{0}	1	5109	88 ± 11	5020 ± 72	3994 ± 112
	2	286	28.3 ± 4.2	258 ± 17	60 ± 11
	3	101	12.5 ± 2.4	88 ± 10	20.5 ± 4.3
	4	26	8.3 ± 1.9	17.7 ± 5.4	4.1 ± 1.4
	5	21	10.3 ± 2.3	10.7 ± 5.1	2.5 ± 1.3
	6	2	$0.23^{+1.10}_{-0.23}$	1.8 ± 1.8	$0.41^{+0.42}_{-0.41}$
N_{5-6}^{0}	7	710	13.4 ± 2.7	697 ± 27	654 ± 45
	8	38	1.99 ± 0.64	36.0 ± 6.2	15.8 ± 4.8
	9	11	2.6 ± 1.0	8.4 ± 3.5	3.7 ± 1.8
	10	4	1.2 ± 0.6	2.8 ± 2.1	1.23 ± 0.97
	11	1	0.84 ± 0.63	$0.2^{+1.2}_{-0.2}$	$0.00^{+0.52}_{-0.00}$
$N_{\geq 7}^{0}$	12	89	2.60 ± 1.0	86.4 ± 9.5	90 ± 17
	13	6	1.56 ± 0.95	4.4 ± 2.6	1.8 ± 1.2
	14	3	$0.06^{+1.1}_{-0.06}$	2.9 ± 2.1	1.22 ± 0.94
	15	1	0.83 ± 0.65	$0.17^{+1.2}_{-0.17}$	0.07 ± 0.50
	16	0	$0.62^{+0.70}_{-0.62}$	$0.0^{+1.8}_{-0.0}$	$0.00^{+0.75}_{-0.00}$
$N_{2-4}^{\geq 1}$	17	1320	37.2 ± 6.4	1283 ± 37	838 ± 48
	18	78	6.3 ± 1.7	71 ± 9	11.3 ± 3.3
	19	39	2.8 ± 1.1	36.2 ± 6.3	5.7 ± 1.8
	20	5	1.2 ± 1.3	3.8 ± 2.6	0.59 ± 0.44
	21	8	2.0 ± 1.1	6.0 ± 3.0	0.95 ± 0.54
$N_{5-6}^{\geq 1}$	22	319	16.8 ± 3.7	302 ± 18	275 ± 31
	23	28	3.4 ± 1.0	24.6 ± 5.4	7.7 ± 2.4
	24	8	1.23 ± 0.61	6.8 ± 2.9	2.1 ± 1.0
	25	2	1.05 ± 0.61	$0.95^{+1.5}_{-0.95}$	$0.30^{+0.49}_{-0.30}$
	26	1	1.19 ± 0.66	$0.0^{+1.8}_{-0.0}$	$0.00^{+0.56}_{-0.00}$
$N_{\geq 7}^{\geq 1}$	27	61	4.2 ± 1.3	56.8 ± 7.9	74 ± 18
	28	12	2.4 ± 1.0	9.6 ± 3.6	5.9 ± 5.0
	29	0	$0.44^{+0.99}_{-0.00}$	$0.0^{+1.8}_{-0.0}$	$0.0^{+1.1}_{-0.0}$
	30	0	0.33 ± 0.99	$0.0^{+1.8}_{-0.0}$	$0.0^{+1.1}_{-0.0}$
	31	0	$0.02^{+1.1}_{-0.00}$	$0.0^{+1.8}_{-0.0}$	$0.0^{+1.1}_{-0.0}$

For thesis